

AFFDL-TR-68-136

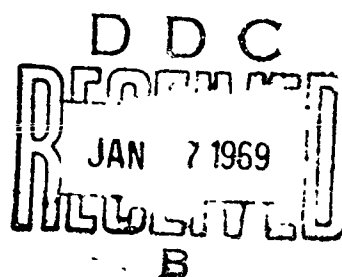
AD 680014

**ON THE INFLUENCE OF INITIAL GEOMETRIC
IMPERFECTIONS ON THE BUCKLING AND POSTBUCKLING
BEHAVIOR OF FIBER-REINFORCED CYLINDRICAL SHELLS
UNDER UNIFORM AXIAL COMPRESSION**

N. S. KHOT

TECHNICAL REPORT AFFDL-TR-68-136

OCTOBER 1968



This document has been approved for public
release and sale; its distribution is unlimited.

**AIR FORCE FLIGHT DYNAMICS LABORATORY
AIR FORCE SYSTEMS COMMAND
WRIGHT-PATTERSON AIR FORCE BASE, OHIO**

Reproduced by the
CLEARINGHOUSE
for Federal Scientific & Technical
Information Springfield Va 22151

NOTICE

When Government drawings, specifications, or other data are used for any purpose other than in connection with a definitely related Government procurement operation, the United States Government thereby incurs no responsibility nor any obligation whatsoever; and the fact that the Government may have formulated, furnished, or in any way supplied the said drawings, specifications, or other data, is not to be regarded by implication or otherwise as in any manner licensing the holder or any other person or corporation, or conveying any rights or permission to manufacture, use, or sell any patented invention that may in any way be related thereto.

This document has been approved for public release and sale; its distribution is unlimited.

ACCESSION NO.	
REPORT	WHITE SECTION <input checked="" type="checkbox"/>
DOC	BUFF SECTION <input type="checkbox"/>
UNANNOUNCED	<input type="checkbox"/>
JUSTIFICATION	
.....	
BY	
DISTRIBUTION/AVAILABILITY CODES	
DIST.	AVAIL. and/or SPECIAL

Copies of this report should not be returned unless return is required by security considerations, contractual obligations, or notice on a specific document.

AFFDL-TR-68-136

**ON THE INFLUENCE OF INITIAL GEOMETRIC
IMPERFECTIONS ON THE BUCKLING AND POSTBUCKLING
BEHAVIOR OF FIBER-REINFORCED CYLINDRICAL SHELLS
UNDER UNIFORM AXIAL COMPRESSION**

N. S. KHOT

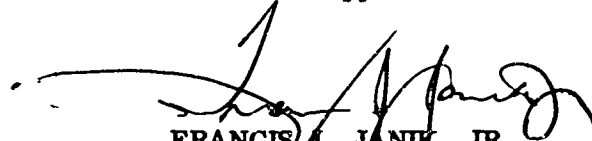
This document has been approved for public
release and sale; its distribution is unlimited.

FOREWORD

This report is prepared as a part of in-house effort under Project No. 1473, "Exploratory Development in Structural Mechanics," Task No. 147306, "Stress and Stability Analysis of Heterogeneous Anisotropic Plates and Shells and Arches." The work was carried out in the Advanced Theory Group and Structural Synthesis Group of the Theoretical Mechanics Branch, Structures Division of the Air Force Flight Dynamics Laboratory, Air Force Systems Command, Wright-Patterson Air Force Base, Ohio. Dr. N. S. Khot (FDTR) was the Project Engineer.

This report covers work conducted during the period September 1967 to May 1968. It was released by the author in August 1968.

This technical report has been reviewed and is approved.



FRANCIS J. JANIK, JR.
Chief, Theoretical Mechanics Branch
Structures Division
Air Force Flight Dynamics Laboratory

ABSTRACT

The effect of initial geometric imperfections on the buckling and postbuckling behavior of composite cylindrical shells are subjected to uniform axial compression is studied in this report. The solution is obtained by employing von Kármán-Donnell nonlinear strain-displacement relations and the principle of stationary potential energy. Numerical results are given for various fiber orientations in the three-layer shell consisting of either glass-epoxy or boron-epoxy composites, with different initial imperfections. Results indicate that the boron-epoxy composite shells are less imperfection sensitive than the glass-epoxy composite shells. Isotropic shells are found to be more imperfection sensitive than composite shells. It is noticed that the increase or decrease in the classical buckling load with change in fiber orientation is generally accompanied by a decrease or increase in imperfection sensitivity of the shell.

TABLE OF CONTENTS

SECTION	PAGE
I INTRODUCTION	1
II PROBLEM FORMULATION	2
1. Strain-Displacement Relations	3
2. Stress Resultants	4
3. Potential Energy	5
4. Equilibrium and Compatible Equations	5
5. Radial Deflection Function, Initial Imperfection and Compatible Stress Function	7
6. Unit End-Shortening and Uniform Radial Dis- placement	11
7. Total Potential Energy	11
8. Nonlinear Algebraic Equations	15
9. Numerical Analysis	17
III RESULTS AND CONCLUSIONS	18
REFERENCES	21

ILLUSTRATIONS

FIGURE		PAGE
1.	Geometry	24
2.	Notation	25
3.	Initial Imperfection Solution of Isotropic Cylinder	26
4.	Initial Imperfection Solution of Glass-Epoxy Composite Cylinder for Fiber Orientation ($0^\circ, 0^\circ, 0^\circ$)	27
5.	Initial Imperfection Solution of Boron-Epoxy Composite Cylinder for Fiber Orientation ($0^\circ, 0^\circ, 0^\circ$)	28
6.	Influence of Initial Imperfection on Buckling Load of Three-layer, Glass-Epoxy Composite Cylinder for Fiber Orientation ($\theta^\circ, -\theta^\circ, 0^\circ$)	29
7.	Imperfection Sensitivity of Three-layer, Glass-Epoxy Composite Cylinder for Fiber Orientation ($\theta^\circ, -\theta^\circ, 0^\circ$)	30
8.	Influence of Initial Imperfection on Buckling Load of Three-layer, Boron-Epoxy Composite Cylinder for Fiber Orientation ($\theta^\circ, -\theta^\circ, 0^\circ$)	31
9.	Imperfection Sensitivity of Three-layer, Boron-Epoxy Composite Cylinder for Fiber Orientation ($\theta^\circ, -\theta^\circ, 0^\circ$)	32
10.	Influence of Initial Imperfection on Buckling Load of Three-layer, Glass-Epoxy Composite Cylinder for Fiber Orientation ($\theta^\circ, -\theta^\circ, 90^\circ$)	33
11.	Imperfection Sensitivity of Three-layer, Glass-Epoxy Composite Cylinder for Fiber Orientation ($\theta^\circ, -\theta^\circ, 90^\circ$)	34
12.	Influence of Initial Imperfection on Buckling Load of Three-layer, Boron-Epoxy Composite Cylinder for Fiber Orientation ($\theta^\circ, -\theta^\circ, 90^\circ$)	35
13.	Imperfection Sensitivity of Three-layer, Boron-Epoxy Composite Cylinder for Fiber Orientation ($\theta^\circ, -\theta^\circ, 90^\circ$)	36

TABLES

TABLE		PAGE
1.	Classical Buckling Loads for Glass-Epoxy Composite Cylindrical Shell	37
2.	Classical Buckling Loads for Boron-Epoxy Composite Cylindrical Shell	38
3.	Buckling Loads for Imperfect Glass-Epoxy Composite Cylindrical Shell for $\bar{W}^* = 0.01$	39
4.	Buckling Loads for Imperfect Glass-Epoxy Composite Cylindrical Shell for $\bar{W}^* = 0.02$	40
5.	Buckling Loads for Imperfect Glass-Epoxy Composite Cylindrical Shell for $\bar{W}^* = 0.04$	41
6.	Buckling Loads for Imperfect Glass-Epoxy Composite Cylindrical Shell for $\bar{W}^* = 0.06$	42
7.	Buckling Loads for Imperfect Glass-Epoxy Composite Cylindrical Shell for $\bar{W}^* = 0.08$	43
8.	Buckling Loads for Imperfect Glass-Epoxy Composite Cylindrical Shell for $\bar{W}^* = 0.10$	44
9.	Buckling Loads for Imperfect Glass-Epoxy Composite Cylindrical Shell for $\bar{W}^* = 0.20$	45
10.	Buckling Loads for Imperfect Glass-Epoxy Composite Cylindrical Shell for $\bar{W}^* = 0.30$	46
11.	Buckling Loads for Imperfect Boron-Epoxy Composite Cylindrical Shell for $\bar{W}^* = 0.01$	47
12.	Buckling Loads for Imperfect Boron-Epoxy Composite Cylindrical Shell for $\bar{W}^* = 0.02$	48
13.	Buckling Loads for Imperfect Boron-Epoxy Composite Cylindrical Shell for $\bar{W}^* = 0.04$	49
14.	Buckling Loads for Imperfect Boron-Epoxy Composite Cylindrical Shell for $\bar{W}^* = 0.06$	50
15.	Buckling Loads for Imperfect Boron-Epoxy Composite Cylindrical Shell for $\bar{W}^* = 0.08$	51
16.	Buckling Loads for Imperfect Boron-Epoxy Composite Cylindrical Shell for $\bar{W}^* = 0.10$	52

TABLES (CONTD)

TABLE		PAGE
17.	Buckling Loads for Imperfect Boron-Epoxy Composite Cylindrical Shell for $\bar{W}^* = 0.20$	53
18.	Buckling Loads for Imperfect Boron-Epoxy Composite Cylindrical Shell for $\bar{W}^* = 0.30$	54

SYMBOLS

$A_{ij} = [A]$	in-plane stiffness matrix
$A_1, A_2, \dots, \bar{A}_1, \bar{A}_2, \dots$	parameters defined in text
$a_{ij} = [a]$	in-plane compliance matrix
$B_1, B_2, \dots, \bar{B}_1, \bar{B}_2, \dots$	parameters defined in text
$C_{ij}^{(k)} = [C^{(k)}]$	anisotropic stiffness matrix associated with k^{th} lamina
$C_1, C_2, \dots, \bar{C}_1, \bar{C}_2, \dots$	parameters defined in text
$D_{ij} = [D]$	stiffness coupling matrix
$d_{ij} = [d]$	compliance coupling matrix
$D_{ij}^* = [D^*]$	bending stiffness matrix
$d_{ij}^* = [d^*]$	modified bending stiffness matrix
E_{11}, E_{12}, E_{22}	elastic constants
N	number of circumferential waves
N_x, N_y, N_{xy}	stress resultants for the entire laminated shell thickness
P_1, P_2, P_3, P_4	modified radial deflection parameters
	$P_i = \frac{W_i}{\sqrt{a_{22} d_{22}^*}} \quad i=1 \text{ through } 4$
$\bar{P}_1, \bar{P}_2, \bar{P}_3, \bar{P}_4$	modified amplitudes of initial imperfection \bar{W}
R	radius of the reference surface of the circular cylindrical shell
S_1, S_2, S_3, \dots T_1, T_2, T_3, \dots	parameters defined in text
U, V, W	reference surface displacements in axial, circumferential and radially inward direction, respectively
\bar{W}^*	imperfection parameter
\bar{W}	initial imperfection of reference surface in radial direction

SYMBOLS (CONTD)

$F(x, y)$	stress function
F_1, F_2, F_3, \dots	stress function parameters defined in text
G_1, G_2, G_3, \dots	parameters defined in text
H_1, H_2, H_3, \dots	parameters defined in text
h_k	the z - coordinate of common boundary of k th and $(k-1)$ th layers as per Figure 1(b)
k_x, k_y, k_{xy}	changes in curvatures
L	length of circular cylindrical shell
ℓ_x, ℓ_y	axial and circumferential half-wave-lengths respectively
M_x, M_y, M_{xy}	moment resultants
n	number of laminas in shell thickness
W_0, W_1, W_2, W_3, W_4	radial deflection parameters
$\bar{W}_1, \bar{W}_2, \bar{W}_3, \bar{W}_4$	amplitudes of initial imperfection \bar{W}
x, y, z	axial circumferential, radial coordinate
$\alpha, \beta, \gamma, \nu, \xi, \kappa, \lambda, \psi, \rho, \phi$	stiffness parameters as defined below

$$\alpha = \frac{2a_{12} + a_{66}}{\sqrt{a_{11} a_{22}}}$$

$$\beta = \frac{a_{26}}{a_{11}^{1/4} a_{22}^{3/4}}$$

$$\gamma = \frac{a_{16}}{a_{11}^{3/4} a_{22}^{1/4}}$$

$$\nu = \frac{2d_{62} - d_{16}}{\sqrt{a_{22} d_{22}^2}} \sqrt{\frac{a_{11}}{a_{22}}}$$

$$\xi = \frac{2d_{61} - d_{28}}{\sqrt{a_{22} d_{22}^2}} \sqrt{\frac{a_{22}}{a_{11}}}$$

SYMBOLS (CONTD)

$$\kappa = \frac{d_{12}}{a_{22}} \sqrt{\frac{a_{11}}{d_{22}^*}}$$

$$\lambda = \frac{d_{21}}{\sqrt{a_{11} d_{22}^*}}$$

$$\psi = \frac{d_{11} + d_{22} - 2d_{66}}{\sqrt{a_{22} d_{22}^*}}$$

$$\rho = \frac{d_{12}^* + 2d_{66}^*}{\sqrt{a_{11}^* a_{22}^*}}$$

$$\phi = \frac{a_{11} d_{11}^*}{a_{22} d_{22}^*}$$

θ fiber orientation (see Figure 1(c))

ϵ end-shortening parameter

$$\epsilon = \frac{\bar{\epsilon} R}{2 \sqrt{a_{11} d_{22}^*}}$$

$\bar{\epsilon}$ end-shortening per unit length (in./in.)

σ average axial compressive unit load parameter

$$\sigma = \frac{\bar{\sigma} R}{2} \sqrt{\frac{a_{11}}{d_{22}^*}}$$

$\bar{\sigma}$ average axial compressive unit load (lb/in.)

$\bar{\sigma}_{\max}$ maximum load an imperfect shell can support before snap-through (lb/in.)

$\bar{\sigma}_{cl}$ classical buckling unit load (lb/in.)

σ_{cl} classical buckling unit load parameter

$$\sigma_{cl} = \frac{\bar{\sigma}_{cl} R}{2} \sqrt{\frac{a_{11}}{d_{22}^*}}$$

SYMBOLS (CONTD)

$\bar{\mu}$ $\frac{\ell_y}{\ell_x}$, wavelength ratio

μ wavelength ratio parameter

$$\mu = \bar{\mu} \sqrt{\frac{\sigma_{22}}{\sigma_{11}}}$$

ω circumferential wave number parameter

$$\omega = \frac{R}{\sqrt{\sigma_{22} d_{22}^N}} \cdot \frac{1}{N^2}$$

ρ^* $\frac{\bar{\sigma}_{\max}}{\bar{\sigma}_{cl}}$

SECTION I

INTRODUCTION

This report is concerned with the influence of initial geometric imperfections on the buckling and postbuckling behavior of laminated anisotropic cylindrical shells. It has been established that geometric imperfections reduce the buckling strength of isotropic cylindrical shells and the extent of the reduction has been studied by many authors (References 1 through 8). A similar reduction in buckling strength due to initial geometric imperfections is expected in the case of the anisotropic cylindrical shells. The increasing use of fiber composite cylinders in aerospace structures prompted this study.

von Kármán-Donnell large-displacement relations, modified to include geometric imperfections, are used in the analysis. The solution to the problem is obtained by the application of the principle of stationary potential energy.

The importance of initial geometric deviations on the buckling behavior of an isotropic shell has been recognized for some time. This can be seen from the early investigations of Flügge (Reference 1) in 1932 and Donnell (Reference 2) in 1934.

However, Flügge's linear and Donnell's nonlinear analyses failed to explain the magnitude of difference between the experimental and the theoretical results. In 1950, Donnell and Wan (Reference 3) changed the procedure adopted by Donnell sixteen years earlier and proposed a new method. This method was followed by several investigators (References 4 through 7) with some modifications.

In the procedure developed by Donnell and Wan, and followed by others, the total potential energy of the system is minimized with respect to the parameters defining the shape of initial deviation of shell geometry. This implies that the shape of the cylinder is altered during minimization of the total potential energy. Madsen and Hoff in Reference 8 were the first to point out the error in this approach. In this investigation, minimization is carried out only with respect to terms of the additional displacement in radial direction caused by the applied load.

The general theory of anisotropic shells was developed by Ambartsumyan (Reference 9) and Dong et al. (Reference 10). Tasi et al. (Reference 11) and Holston, et al. (Reference 12) investigated the buckling strength of filament wound cylinders where they used the small-deflection analysis presented by Chang and Ho (References 13 and 14). The effect of heterogeneity on the stability of composite shells subjected to axial compression is investigated by Tasi (Reference 15). Thurston (Reference 16) outlined a large-displacement analysis of filament wound cylinders under axial compression, where he proposes to solve the two non-linear partial differential equations by Newton's method. The effect of fiber orientation on buckling and postbuckling behavior of geometrically perfect fiber-reinforced cylinders under axial compression is investigated by Khot (Reference 17).

The numerical results presented in this report are for the geometrically imperfect three-layer glass-epoxy and boron-epoxy composite cylindrical shells.

SECTION II

PROBLEM FORMULATION

The coordinate system employed on the reference surface is shown in Figure 1; x is taken parallel to the generator, y is measured along the circumference, and z is positive in the inward direction.

1. STRAIN-DISPLACEMENT RELATIONS

The reference surface nonlinear strain-displacement relations based on the work of Donnell (Reference 2) for a cylindrical shell of radius R with initial radial imperfections \bar{W} are given by

$$\begin{aligned}\epsilon_x &= U_{,x} + \frac{1}{2} (W_{,x})^2 - \frac{1}{2} (\bar{W}_{,x})^2 \\ \epsilon_y &= V_{,y} + \frac{1}{2} (W_{,y})^2 - \frac{1}{2} (\bar{W}_{,y})^2 - \frac{1}{R} (W - \bar{W}) \\ \epsilon_{xy} &= V_{,x} + U_{,y} + W_{,x} W_{,y} - \bar{W}_{,x} \bar{W}_{,y}\end{aligned}\quad (1)$$

where U , V , and W are the components of the reference surface displacement vector, and \bar{W} is the initial deviation of the shell in inward direction from a circular cylindrical shape. W is the total displacement in the radial direction including \bar{W} . Then $(W - \bar{W})$ is the displacement produced by the applied load only. The total strains are then given by

$$\begin{aligned}\mathcal{E}_x &= \epsilon_x - zk_x \\ \mathcal{E}_y &= \epsilon_y - zk_y \\ \mathcal{E}_{xy} &= \epsilon_{xy} - zk_{xy}\end{aligned}\quad (2)$$

where

$$\begin{aligned}k_x &= W_{,xx} - \bar{W}_{,xx} \\ k_y &= W_{,yy} - \bar{W}_{,yy} \\ k_{xy} &= 2(W_{,xy} - \bar{W}_{,xy})\end{aligned}\quad (3)$$

2. STRESS RESULTANTS

The relations between resultant stresses and strains for the entire laminated wall are written as (References 10 and 18)

$$[N] = [A][\epsilon] - [D][k] \quad (4)$$

$$[M] = [D][\epsilon] - [D^*][k] \quad (5)$$

where the elements of (3×3) matrices $[A]$, $[D]$, and $[D^*]$ are given by

$$A_{ij} = \sum_{k=1}^n C_{ij}^{(k)} (h_{k+1} - h_k)$$

$$D_{ij} = \frac{1}{2} \sum_{k=1}^n C_{ij}^{(k)} (h_{k+1}^2 - h_k^2)$$

$$D_{ij}^* = \frac{1}{3} \sum_{k=1}^n C_{ij}^{(k)} (h_{k+1}^3 - h_k^3)$$

In the above definitions n is the number of laminae, k denotes the k^{th} layer bounded by z -coordinates h_k and h_{k+1} (Figure 1(b)), and $C_{ij}^{(k)}$ is the anisotropic stiffness matrix associated with the k^{th} lamina. Inversion of Equation 4 and substitution into Equation 5 yield

$$[\epsilon] = [a][N] + [d'][k] \quad (6)$$

$$[M] = [d][N] - [d^*][k]$$

where

$$[a] = [A]^{-1} \quad [d] = [D][a]$$

$$[d'] = [a][D] = [d]^T$$

$$[d^*] = [D^*] - [D][a][D]$$

3. POTENTIAL ENERGY

The total strain energy of a multilayered cylindrical shell of radius R and length L can be expressed as the sum of the following two expressions (Reference 17)

$$\begin{aligned} \Pi_1 = \frac{1}{2} \int_0^L \int_0^{2\pi R} & (a_{11} N_x^2 + a_{22} N_y^2 + a_{66} N_{xy}^2 + 2a_{12} N_x N_y \\ & + 2a_{16} N_x N_{xy} + 2a_{26} N_y N_{xy}) dx dy \end{aligned} \quad (7)$$

$$\begin{aligned} \Pi_2 = \frac{1}{2} \int_0^L \int_0^{2\pi R} & (d_{11}^* k_x^2 + d_{22}^* k_y^2 + d_{66}^* k_{xy}^2 + 2d_{12}^* k_x k_y \\ & + 2d_{16}^* k_x k_{xy} + 2d_{26}^* k_y k_{xy}) dx dy \end{aligned} \quad (8)$$

The energy associated with the work done by the uniformly applied axial compressive end load is given by

$$\Pi_3 = - \int_0^{2\pi R} \left[N_x \right]_{x=L} dy \int_0^L U_{,x} dx \quad (9)$$

The total potential energy is then given by

$$\Pi = \Pi_1 + \Pi_2 + \Pi_3 \quad (10)$$

4. EQUILIBRIUM AND COMPATIBILITY EQUATIONS

The equilibrium equations resulting from the first variation of the total potential energy with respect to the displacements U , V and W are given by

$$N_{x,x} + N_{xy,y} = 0 \quad (11)$$

$$N_{xy,x} + N_{y,y} = 0$$

$$\begin{aligned} \frac{N_y}{R} + N_x (W_{,xx} - \bar{W}_{,xx}) + 2N_{xy} (W_{,xy} - \bar{W}_{,xy}) + N_y (W_{,yy} - \bar{W}_{,yy}) \\ + M_{x,xx} + 2M_{xy,xy} + M_{y,yy} = 0 \end{aligned} \quad (12)$$

The three unknowns in Equation 11 can be replaced by a single unknown $F(x,y)$, the Airy stress function, which is defined as

$$\begin{aligned} N_x &= F_{,yy} \\ N_y &= F_{,xx} \\ N_{xy} &= -F_{,xy} \end{aligned} \quad (13)$$

Utilizing Equations 6 and 13 in Equation 12 the equilibrium equation in radial direction can be written as

$$\begin{aligned} d_{12} F_{,xxxx} + (2d_{62} - d_{18}) F_{,xxxy} + (d_{11} + d_{22} - 2d_{66}) F_{,xxyy} \\ + (2d_{61} - d_{26}) F_{,xyyy} + d_{21} F_{,yyyy} + F_{,xx} (W_{,yy} + \frac{1}{R}) + F_{,yy} W_{,xx} \\ - 2F_{,xy} W_{,xy} - d_{11}^* (W_{,xxxx} - \bar{W}_{,xxxx}) - 4d_{16}^* (W_{,xxxy} - \bar{W}_{,xxxy}) \\ - (2d_{12}^* + 4d_{66}^*) (W_{,xxyy} - \bar{W}_{,xxyy}) - 4d_{26}^* (W_{,xyyy} - \bar{W}_{,xyyy}) \\ - d_{22}^* (W_{,yyyy} - \bar{W}_{,yyyy}) = 0 \end{aligned} \quad (14)$$

Eliminating U and V from Equation 1 the compatibility condition can be written as

$$\begin{aligned} \epsilon_{x,yy} + \epsilon_{y,xx} - \epsilon_{xy,xy} &= (W_{,xy})^2 - W_{,xx} W_{,yy} - \frac{1}{R} W_{,xx} \\ &\quad - (\bar{W}_{,xy})^2 + \bar{W}_{,xx} \bar{W}_{,yy} + \frac{1}{R} \bar{W}_{,xx} \end{aligned} \quad (15)$$

The above equation can be expressed in terms of stress function by utilizing Equations 6 and 13 as follows

$$\begin{aligned} d_{22} F_{,xxxx} - 2d_{66} F_{,xxxy} + (2d_{12} + d_{66}) F_{,xxyy} - 2d_{16} F_{,xyyy} \\ + d_{11} F_{,yyyy} &= -d_{12} (W_{,xxxx} - \bar{W}_{,xxxx}) - (2d_{62} - d_{18}) (W_{,xxxy} - \bar{W}_{,xxxy}) \\ &\quad - (d_{11} + d_{22} - 2d_{66}) (W_{,xxyy} - \bar{W}_{,xxyy}) - (2d_{61} - d_{26}) (W_{,xyyy} \\ &\quad - \bar{W}_{,xyyy}) - d_{21} (W_{,yyyy} - \bar{W}_{,yyyy}) + (W_{,xy})^2 - (\bar{W}_{,xy})^2 \\ &\quad - (W_{,xx} W_{,yy} - \bar{W}_{,xx} \bar{W}_{,yy}) - (\frac{1}{R} W_{,xx} - \frac{1}{R} \bar{W}_{,xx}) \end{aligned} \quad (16)$$

5. RADIAL DEFLECTION FUNCTION, INITIAL IMPERFECTION, AND COMPATIBLE STRESS FUNCTION

The following trigonometric expressions are used to represent the total radial displacement, W and initial radial imperfection, \bar{W}

$$W = W_1 \cos \frac{\pi x}{\ell_x} \cos \frac{\pi y}{\ell_y} + W_2 \cos \frac{2\pi x}{\ell_x} + W_3 \cos \frac{2\pi x}{\ell_x} \cos \frac{2\pi y}{\ell_y} + W_4 \cos \frac{4\pi x}{\ell_x} + W_0 \quad (17)$$

$$\bar{W} = \bar{W}_1 \cos \frac{\pi x}{\ell_x} \cos \frac{\pi y}{\ell_y} + \bar{W}_2 \cos \frac{2\pi x}{\ell_x} + \bar{W}_3 \cos \frac{2\pi x}{\ell_x} \cos \frac{2\pi y}{\ell_y} + \bar{W}_4 \cos \frac{4\pi x}{\ell_x} \quad (18)$$

where W_0 through W_4 are the unknown coefficients in the radial displacement function and \bar{W}_1 through \bar{W}_4 are the amplitudes of the imperfections. ℓ_x and ℓ_y are the half-wavelengths in the axial and circumferential directions.

Equation 17, assumed to represent the total radial displacement, is of the same form as that used for investigating the postbuckling behavior of geometrically perfect anisotropic shells in Reference 17, and for isotropic shells in Reference 19. In the selection of the buckling configuration (Equation 17), assumption is made that the shell may not deform into a torsional buckling mode.

Substitution of the expressions for the assumed deflected shape and initial imperfection into the compatibility equation and subsequent solution yield the following expression for the stress function

$$F = \bar{F} - \frac{\bar{\sigma}_y^2}{2} \quad (19)$$

in which $\bar{\sigma}$ is the applied axial compressive load and the expression for \bar{F} is as given below

$$\begin{aligned}
 \bar{F} = & F_1 \cos \frac{\pi x}{\ell_x} \cos \frac{\pi y}{\ell_y} + F_2 \sin \frac{\pi x}{\ell_x} \sin \frac{\pi y}{\ell_y} + F_3 \cos \frac{2\pi x}{\ell_x} + F_4 \cos \frac{2\pi y}{\ell_y} \\
 & + F_5 \cos \frac{2\pi x}{\ell_x} \cos \frac{2\pi y}{\ell_y} + F_6 \sin \frac{2\pi x}{\ell_x} \sin \frac{2\pi y}{\ell_y} + F_7 \cos \frac{3\pi x}{\ell_x} \cos \frac{\pi y}{\ell_y} \\
 & + F_8 \sin \frac{3\pi x}{\ell_x} \sin \frac{\pi y}{\ell_y} + F_9 \cos \frac{\pi x}{\ell_x} \cos \frac{3\pi y}{\ell_y} + F_{10} \sin \frac{\pi x}{\ell_x} \sin \frac{3\pi y}{\ell_y} \\
 & + F_{11} \cos \frac{4\pi x}{\ell_x} + F_{12} \cos \frac{4\pi y}{\ell_y} + F_{13} \cos \frac{4\pi x}{\ell_x} \cos \frac{2\pi y}{\ell_y} \\
 & + F_{14} \sin \frac{4\pi x}{\ell_x} \sin \frac{2\pi y}{\ell_y} + F_{15} \cos \frac{5\pi x}{\ell_x} \cos \frac{\pi y}{\ell_y} + F_{16} \sin \frac{5\pi x}{\ell_x} \sin \frac{\pi y}{\ell_y} \\
 & + F_{17} \cos \frac{6\pi x}{\ell_x} \cos \frac{2\pi y}{\ell_y} + F_{18} \sin \frac{6\pi x}{\ell_x} \sin \frac{2\pi y}{\ell_y} \quad (20)
 \end{aligned}$$

where the parameters F_1 through F_{18} which are the functions of parameters W_1 through W_4 and \bar{W}_1 through \bar{W}_4 , are as given below

$$\begin{aligned}
 F_1 = & \frac{-\left\{ \bar{A}_1 \left(G_1 - \frac{\ell_y^2}{R\pi^2} \right) - 2\bar{B}_1 \right\} \{ G_2 \} - \bar{A}_1 G_3 G_4}{G_2^2 - G_4^2} \\
 F_2 = & \frac{\bar{A}_1 G_3 G_2 + \left\{ \bar{A}_1 \left(G_1 - \frac{\ell_y^2}{R\pi^2} \right) + 2\bar{B}_1 \right\} G_4}{G_2^2 - G_4^2} \\
 F_3 = & \bar{A}_2 \left\{ -\frac{d_{12}}{a_{22}} + \frac{\frac{\ell_y^2}{4\mu^2 a_{22} R\pi^2}}{\frac{\ell_y^2}{4\mu^2 a_{22} R\pi^2}} \right\} - \frac{\bar{C}_1}{32\mu^2 a_{22}} \\
 F_4 = & \bar{C}_1 \left\{ -\frac{1}{32\eta^2 a_{11}} \right\} + \bar{B}_5 \left\{ -\frac{1}{2\eta^2 a_{11}} \right\} \\
 F_8 = & \frac{\left\{ -\bar{A}_3 \left(G_1 - \frac{\ell_y^2}{4R\pi^2} \right) - 2\bar{B}_2 \right\} - \bar{A}_3 G_3 G_4}{G_2^2 - G_4^2} \quad (21)
 \end{aligned}$$

$$F_6 = \frac{\bar{A}_3 G_3 G_2 + \left\{ \bar{A}_3 \left(G_1 - \frac{\ell_y^2}{4 R \pi^2} \right) - 2 \bar{B}_2 \right\} G_4}{G_2^2 - G_8^2}$$

$$F_7 = - \left\{ 4 \bar{B}_3 + 2 \bar{B}_1 + 8 \bar{B}_4 \right\} G_5 / (G_5^2 - G_6^2)$$

$$F_8 = \left\{ 4 \bar{B}_3 + 2 \bar{B}_1 + 8 \bar{B}_4 \right\} G_6 / (G_5^2 - G_6^2)$$

$$F_9 = -4 \bar{B}_3 G_7 / (G_7^2 - G_8^2)$$

$$F_{10} = 4 \bar{B}_3 G_8 / (G_7^2 - G_8^2)$$

$$F_{11} = \bar{A}_4 \left\{ -\frac{d_{12}}{a_{22}} + \frac{\ell_y^2}{16 \bar{\mu}^2 a_{22} \pi^2 R} \right\} - \frac{\bar{C}_3}{32 \bar{\mu}^2 a_{22}}$$

$$F_{12} = -\bar{C}_3 / 32 \bar{\eta}^2 a_{11}$$

$$F_{13} = -\bar{B}_5 G_9 / (G_9^2 - G_{10}^2)$$

$$F_{14} = \bar{B}_5 G_{10} / (G_9^2 - G_{10}^2)$$

$$F_{15} = -8 \bar{B}_4 G_{11} / (G_{11}^2 - G_{12}^2)$$

$$F_{16} = 8 \bar{B}_4 G_{12} / (G_{11}^2 - G_{12}^2)$$

$$F_{17} = -2 \bar{B}_2 G_{13} / (G_{13}^2 - G_{14}^2)$$

$$F_{18} = 2 \bar{B}_2 G_{14} / (G_{13}^2 - G_{14}^2)$$

$$\bar{\mu} = \frac{\ell_y}{\ell_x}$$

$$\bar{\eta} = \frac{\ell_x}{\ell_y}$$

$$\bar{A}_1 = W_1 - \bar{W}_1$$

$$\bar{A}_2 = W_2 - \bar{W}_2$$

$$\bar{A}_3 = W_3 - \bar{W}_3$$

$$\bar{A}_4 = W_4 - \bar{W}_4$$

$$\overline{B}_1 = W_1 W_2 - \overline{W}_1 \overline{W}_2$$

$$\overline{B}_2 = W_3 W_4 - \overline{W}_3 \overline{W}_4$$

$$\overline{B}_3 = W_1 W_3 - \overline{W}_1 \overline{W}_3$$

$$\overline{B}_4 = W_1 W_4 - \overline{W}_1 \overline{W}_4$$

$$\overline{C}_1 = W_1^2 - \overline{W}_1^2$$

$$\overline{C}_3 = W_3^2 - \overline{W}_3^2$$

$$G_1 = d_{12} \overline{\mu}^2 + d_{21} \overline{\eta}^2 + (d_{11} + d_{22} - 2d_{66})$$

$$G_2 = a_{22} \overline{\mu}^2 + a_{11} \overline{\eta}^2 + (2a_{12} + a_{66})$$

$$G_3 = (2d_{62} - d_{16}) \overline{\mu} + (2d_{61} - d_{26}) \overline{\eta}$$

$$G_4 = 2\overline{\mu} a_{26} + 2\overline{\eta} a_{16}$$

$$G_5 = 81a_{22} \overline{\mu}^2 + a_{11} \overline{\eta}^2 + 9(2a_{12} + a_{66})$$

$$G_6 = 54\overline{\mu} a_{26} + 6\overline{\eta} a_{16}$$

$$G_7 = a_{22} \overline{\mu}^2 + 81a_{11} \overline{\eta}^2 + 9(2a_{12} + a_{66})$$

$$G_8 = 6\overline{\mu} a_{26} + 54\overline{\eta} a_{16}$$

$$G_9 = 32a_{22} \overline{\mu}^2 + 2a_{11} \overline{\eta}^2 + 8(2a_{12} + a_{66})$$

$$G_{10} = 32\overline{\mu} a_{26} + 8\overline{\eta} a_{16}$$

$$G_{11} = 625a_{22} \overline{\mu}^2 + a_{11} \overline{\eta}^2 + 25(2a_{12} + a_{66})$$

$$G_{12} = 250\overline{\mu} a_{26} + 10\overline{\eta} a_{16}$$

$$G_{13} = 81a_{22} \overline{\mu}^2 + a_{11} \overline{\eta}^2 + 9(2a_{12} + a_{66})$$

$$G_{14} = 54a_{26} \overline{\mu} + 6a_{16} \overline{\eta}$$

6. UNIT END-SHORTENING AND UNIFORM RADIAL DISPLACEMENT

The unit end-shortening caused by the uniformly applied compressive end load is given by

$$\bar{\epsilon} = -\frac{1}{L} \int_0^L u_{,x} dx \quad (22)$$

then, through utilization of Equations 1, 17, 18, and 19, and integrating Equation 22 end-shortening can be written as

$$\begin{aligned} \bar{\epsilon} = a_{11}\bar{\sigma} + \left[(w_1^2 - \bar{w}_1^2) + 8(w_2^2 - \bar{w}_2^2) \right. \\ \left. + 4(w_3^2 - \bar{w}_3^2) + 32(w_4^2 - \bar{w}_4^2) \right] \frac{\pi^2}{8\ell_x^2} \end{aligned} \quad (23)$$

The continuity condition for the circumferential displacement is given by

$$\begin{aligned} \int_0^{2\pi R} v_{,y} dy = \int_0^{2\pi R} \left[a_{12}F_{,yy} + a_{22}F_{,xx} - a_{26}F_{,xy} + d_{12}W_{,xx} + d_{22}W_{,yy} \right. \\ \left. + 2d_{62}W_{,xy} - \frac{1}{2}(W_{,y})^2 + \frac{1}{2}(\bar{W}_{,y})^2 + \frac{W}{R} - \frac{\bar{W}}{R} \right] dy = 0 \end{aligned} \quad (24)$$

Substitution of the assumed radial deflection function, initial imperfection and stress function into the continuity condition yields the following expression for W_0

$$W_0 = R a_{12}\bar{\sigma} + \left[(w_1^2 - \bar{w}_1^2) + 4(w_3^2 - \bar{w}_3^2) \right] \frac{\pi^2 R}{8\ell_y^2} \quad (25)$$

7. TOTAL POTENTIAL ENERGY

Utilizing Equations 17 through 25, the following expression for the total potential energy is obtained

$$\begin{aligned}
 \Pi \frac{4R}{\pi L d_{22}^*} = & \frac{1}{\omega^2} \left[\frac{T_1}{T_1^2 - T_2^2} \left\{ T_3^2 A_1^2 + 16 T_{13}^2 A_3^2 + T_4^2 A_1^2 + 16 A_3^2 \right\} + 4 T_3 A_1 B_1 \mu^2 \right. \\
 & + 64 T_{13} A_3 B_2 \mu^2 + 4 B_1^2 \mu^4 + 64 B_2^2 \mu^4 \left. \right\} + \frac{T_2 T_4}{T_1^2 - T_2^2} \left\{ 2 T_3 A_1^2 \right. \\
 & + 32 T_{13} A_3^2 + 4 A_1 B_1 \mu^2 + 64 A_3 B_2 \mu^2 \left. \right\} + \frac{T_6}{T_8^2 - T_6^2} \left\{ (4 B_3 \right. \\
 & + 2 B_1 + 8 B_4)^2 + 64 B_2^2 \left. \right\} \mu^4 + \frac{T_7}{T_7^2 - T_8^2} 16 B_3^2 \mu^4 \\
 & + \frac{T_9}{T_9^2 - T_{10}^2} 64 B_4^2 \mu^4 + \frac{T_{11}}{T_{11}^2 - T_{12}^2} 4 B_5^2 \mu^4 + 2 A_2^2 \omega^2 + 2 A_4^2 \omega^2 \\
 & + \frac{1}{32} C_1^2 + \frac{1}{2} C_3^2 - \frac{1}{2} C_1 A_2 \omega - 2 C_3 A_4 \omega + A_1^2 + 16 A_3^2 \\
 & + \left\{ 32 A_2^2 \kappa^2 + 512 A_4^2 \kappa^2 + \frac{1}{32} C_1^2 + \frac{1}{2} C_3^2 + 8 B_5^2 + C_1 B_5 \right. \\
 & + A_1^2 \phi + 32 A_2^2 \phi + 16 A_3^2 \phi + 512 A_4^2 \phi \left. \right\} \mu^4 - \kappa (A_2^2 + 4 A_4^2) 16 \omega \mu^2 \\
 & + \kappa (A_2 C_1 + 16 A_4 C_3) 2 \mu^2 + \rho \sqrt{\phi} (A_1^2 + 32 A_3^2) 2 \mu^2 \\
 & - \left\{ C_1 + 8 C_2 + 4 C_3 + 32 C_4 \right\} 2 \sigma \mu^2 \omega \left. \right] + \text{constants} \quad (26)
 \end{aligned}$$

where

$$\begin{aligned}
 P_i &= \frac{W_i}{(a_{22} d_{22}^*)^{1/2}} & \bar{P}_i &= \frac{\bar{W}_i}{(a_{22} d_{22}^*)^{1/2}} \quad i = 1 \text{ through } 4 \\
 \mu &= \frac{l_y}{l_x} \left(\frac{a_{22}}{a_{11}} \right)^{1/4} & \omega &= \frac{R}{(a_{22} d_{22}^*)^{1/2}} \frac{1}{N^2} \\
 N &= \frac{\pi R}{l_y} & \sigma &= \frac{\bar{\sigma} R}{2} \left(\frac{a_{11}}{d_{22}^*} \right)^{1/2}
 \end{aligned} \quad (27)$$

$$A_1 = P_1 - \bar{P}_1$$

$$A_2 = P_2 - \bar{P}_2$$

$$A_3 = P_3 - \bar{P}_3$$

$$A_4 = P_4 - \bar{P}_4$$

$$B_1 = P_1 P_2 - \bar{P}_1 \bar{P}_2$$

$$B_2 = P_3 P_4 - \bar{P}_3 \bar{P}_4$$

$$B_3 = P_1 P_3 - \bar{P}_1 \bar{P}_3$$

$$B_4 = P_1 P_4 - \bar{P}_1 \bar{P}_4$$

$$B_5 = P_2 P_3 - \bar{P}_2 \bar{P}_3$$

$$C_1 = P_1^2 - \bar{P}_1^2$$

$$C_2 = P_2^2 - \bar{P}_2^2$$

$$C_3 = P_3^2 - \bar{P}_3^2$$

$$C_4 = P_4^2 - \bar{P}_4^2$$

The values of T_1 through T_{13} appearing in the energy expression are as follows

$$T_1 = \mu^4 + \alpha \mu^2 + 1$$

$$T_8 = 6\mu(\mu^2\beta + 9\gamma)$$

$$T_2 = 2\mu(\mu^2\beta + \gamma)$$

$$T_9 = 625\mu^4 + 25\alpha\mu^2 + 1$$

$$T_3 = \kappa\mu^4 + \psi\mu^2 + \lambda - \mu^2\omega$$

$$T_{10} = 10\mu(25\mu^2\beta + \gamma)$$

$$T_4 = \mu(\nu\mu^2 + \xi)$$

$$T_{11} = 16\mu^4 + 4\alpha\mu^2 + 1$$

$$T_5 = 81\mu^4 + 9\alpha\mu^2 + 1$$

$$T_{12} = 4\mu(4\mu^2\beta + \gamma)$$

$$T_6 = 6\mu(9\mu^2\beta + \gamma)$$

$$T_{13} = \kappa\mu^4 + \psi\mu^2 + \lambda - \frac{\omega}{4}\mu^2$$

$$T_7 = \mu^4 + 9\alpha\mu^2 + 1$$

where the stiffness parameters α, β , etc. are defined by the following relations

$$\alpha = \frac{2a_{12} + a_{66}}{\sqrt{a_{11} a_{22}}}$$

$$\beta = \frac{a_{26}}{a_{11}^{1/4} a_{22}^{3/4}}$$

$$\begin{aligned}
\gamma &= \frac{a_{16}}{a_{22}^{1/4} a_{11}^{3/4}} \\
\nu &= \frac{2d_{62} - d_{16}}{\sqrt{a_{22} d_{22}^*}} \sqrt{\frac{a_{11}}{a_{22}}} \\
\xi &= \frac{2d_{61} - d_{26}}{\sqrt{a_{22} d_{22}^*}} \sqrt{\frac{a_{22}}{a_{11}}} \\
\kappa &= \frac{d_{12}}{a_{22}} \sqrt{\frac{a_{11}}{d_{22}^*}} \\
\lambda &= \frac{d_{21}}{\sqrt{a_{11} d_{22}^*}} \\
\psi &= \frac{d_{11} + d_{22} - 2d_{66}}{\sqrt{a_{11} d_{22}^*}} \\
\rho &= \frac{d_{12}^* + 2d_{66}^*}{\sqrt{d_{11}^* d_{22}^*}} \\
\phi &= \frac{a_{11} d_{11}^*}{a_{22} d_{22}^*}
\end{aligned} \tag{28}$$

The end-shortening $\bar{\epsilon}$ (Equation 23) may be redefined as a new parameter

$$\begin{aligned}
\epsilon = \sigma + \frac{1}{16} \left[(P_1^2 - \bar{P}_1^2) + 8(P_2^2 - \bar{P}_2^2) + 4(P_3^2 - \bar{P}_3^2) \right. \\
\left. + 32(P_4^2 - \bar{P}_4^2) \right] \frac{\mu^2}{\omega} \tag{29}
\end{aligned}$$

where

$$\epsilon = \frac{\bar{\epsilon} R}{2 \sqrt{a_{11} d_{22}^*}} \tag{30}$$

8. NONLINEAR ALGEBRAIC EQUATIONS

The condition that for a given σ (i.e., applied axial compressive load) the total potential energy has a stationary value for small variation of P_1, P_2, P_3, P_4 is equivalent to

$$\frac{\partial V}{\partial P_1} = \frac{\partial V}{\partial P_2} = \frac{\partial V}{\partial P_3} = \frac{\partial V}{\partial P_4} = 0 \quad (31)$$

This yields the following four nonlinear algebraic equations

$$\begin{aligned} & \frac{T_1}{T_1^2 - T_2^2} \left\{ 2(T_3^2 + T_4^2)A_1 + 4T_3(B_1 + A_1P_2)\mu^2 + 8B_1P_2\mu^4 \right\} \\ & + \frac{T_2T_4}{T_1^2 - T_2^2} \left\{ 4T_3A_1 + 4\mu^2(B_1 + A_1P_2) \right\} + \frac{T_5}{T_5^2 - T_6^2} \left\{ 2(4B_3 + 2B_1 \right. \\ & + 8B_4)(4P_3 + 2P_2 + 8P_4)\mu^4 \left. \right\} + \frac{T_7}{T_7^2 - T_8^2} 32B_3P_3\mu^4 \\ & + \frac{T_9}{T_9^2 - T_{10}^2} 128B_4P_4\mu^4 + \frac{C_1P_1}{8} - P_1A_2\omega + 2A_1 + \left\{ \frac{C_1P_1}{8} + 2P_1B_5 \right. \\ & + 2A_1\phi \left. \right\} \mu^4 + 4\kappa A_2P_1\mu^2 + 4\rho\sqrt{\phi}A_1\mu^2 - 4P_1\sigma\mu^2\omega = 0 \\ & \frac{T_1}{T_1^2 - T_2^2} \left\{ 4T_3A_1P_1\mu^2 + 8B_1P_1\mu^4 \right\} + \frac{T_2T_4}{T_1^2 - T_2^2} 4A_1P_1\mu^2 \\ & + \frac{T_5}{T_5^2 - T_6^2} \left\{ 8P_1(2B_3 + B_1 + 4B_4)\mu^4 \right\} + \frac{T_{11}}{T_{11}^2 - T_{12}^2} 8B_5P_3\mu^4 + 4A_2\omega^2 \\ & - \frac{C_1\omega}{2} + \left\{ 64A_2\kappa^2 + 16B_5P_3 + C_1P_3 + 64A_2\phi \right\} \mu^4 - 32\kappa A_2\omega\mu^2 \\ & + 2\kappa C_1\mu^2 - 32P_2\sigma\mu^2\omega = 0 \end{aligned}$$

$$\begin{aligned}
 & \frac{T_1}{T^2 - T^2} \left\{ 32 A_3 (T_{13}^2 + T_4^2) + 64 T_{13} \mu^2 (B_2 + A_3 P_4) + 128 B_2 P_4 \mu^4 \right\} \\
 & + \frac{T_2 T_4}{T_1^2 - T_2^2} \left\{ 64 T_{13} A_3 + 64 \mu^2 (B_2 + A_3 P_4) \right\} + \frac{T_5}{T_5^2 - T_6^2} \left\{ 16 (2 B_3 + B_1 \right. \\
 & + 4 B_4) P_1 + 128 B_2 P_4 \left. \right\} \mu^4 + \frac{T_7}{T_7^2 - T_8^2} 32 B_3 P_1 \mu^4 + \frac{T_{11}}{T_{11}^2 - T_{12}^2} 8 B_5 P_2 \mu^4 \\
 & + 64 \kappa A_4 P_3 \mu^2 + 2 C_3 P_3 - 4 A_4 P_3 \omega + 32 A_3 + \left\{ 2 C_3 P_3 + 16 B_5 P_2 + C_1 P_2 \right. \\
 & + 32 A_3 \phi \left. \right\} \mu^4 + 128 \rho \sqrt{\phi} A_3 \mu^2 - 16 P_3 \sigma \mu^2 \omega = 0
 \end{aligned}$$

$$\begin{aligned}
 & \frac{T_1}{T_1^2 - T_2^2} \left\{ 64 T_{13} A_3 P_3 \mu^2 + 128 B_2 P_3 \mu^4 \right\} + \frac{T_2 T_4}{T_1^2 - T_2^2} 64 A_3 P_3 \mu^2 \\
 & + \frac{T_5}{T_5^2 - T_6^2} \left\{ 32 (2 B_3 + B_1 + 4 B_4) P_1 + 128 B_2 P_3 \right\} \mu^4 \\
 & + \frac{T_9}{T_9^2 - T_{10}^2} 128 B_4 P_1 \mu^4 + 4 A_4 \omega^2 - 2 C_3 \omega + \left\{ \kappa^2 + \phi \right\} 1024 A_4 \mu^4 \\
 & - 128 \kappa A_4 \omega \mu^2 + 32 \kappa C_3 \mu^2 - 128 \sigma \mu^2 \omega P_1 = 0
 \end{aligned}$$

The imperfection sensitivity of a cylindrical shell can be measured by a quantity ρ^* which is defined as the ratio of the buckling load of an initially imperfect shell to the classical buckling load. If σ_{\max} is considered as the buckling load of the imperfect shell and $\sigma_{c\ell}$ its classical buckling load then

$$\rho^* = \frac{\sigma_{\max}}{\sigma_{c\ell}} \quad (32)$$

For small imperfections the cylindrical shell passes through a maximum load σ_{\max} state before it snaps through. In case of large imperfections however, the cylinder does not experience snap-through and hence σ_{\max} is not well defined (see Figure 2). For a given shell σ_{\max} depends upon imperfection parameters \bar{P}_1 through \bar{P}_4 , μ , and ω .

The values of deflection parameters P_1 through P_4 can be obtained by solving Equation 32. The solution of this set of equations depends upon the parameters α through ϕ (stiffness), \bar{P}_1 through \bar{P}_4 (initial imperfection amplitudes), μ (aspect ratio), ω (circumferential wave number) and σ (applied axial load). End-shortening ϵ corresponding to the applied load σ can be calculated from Equation 29. The stiffness parameters α through ϕ can be calculated knowing the thickness of the shell, number of layers and the elastic properties of material in each layer (Reference 17). \bar{P}_1 through \bar{P}_4 depend upon the amplitudes of assumed deviations from the geometrically perfect cylindrical shell. The parameters μ and ω depend upon the wavelengths of assumed initial geometric imperfection. For isotropic cylindrical shells Koiter (Reference 20), Hutchinson (Reference 21), and Madsen and Hoff (Reference 8) predicted that the imperfections with wavelengths equal to those for small-deflection buckling mode are most critical. The parameters μ and ω for anisotropic cylindrical shells corresponding to buckling mode for small-deflection theory can be calculated from equations given in Reference 17.

9. NUMERICAL ANALYSIS

The set of nonlinear algebraic equations (Equation 32) can be solved by Newton-Raphson iterative technique (Reference 22). A FORTRAN IV computer program was written for IBM 7094 to solve the equations and to evaluate ϵ for given σ , or σ for given ϵ .

SECTION III

RESULTS AND CONCLUSIONS

From the theoretical analysis developed in the previous sections, it is seen that the behavior of the cylindrical shell depends upon ten stiffness parameters α , β , etc. Because of this large number of parameters, it is not possible to present meaningful general results in terms of stiffness parameters. Accordingly, a three-layer cylindrical shell of radius 6.0 inches and thickness 0.036 inch is selected to illustrate the application of the theory and to arrive at conclusive results. The thickness of each layer is 0.012 inch and all layers consist of either glass-epoxy or boron-epoxy composites. The elastic constants of the composites are as given below.

glass - epoxy	boron - epoxy
$E_{11} = 7.5 \times 10^6 \text{ psi}$	$E_{11} = 40.0 \times 10^6 \text{ psi}$
$E_{22} = 3.5 \times 10^6 \text{ psi}$	$E_{22} = 4.5 \times 10^6 \text{ psi}$
$\nu_{12} = 0.25$	$\nu_{12} = 0.25$
$G = 1.25 \times 10^6 \text{ psi}$	$G = 1.5 \times 10^6 \text{ psi}$
$\nu_{21} = \nu_{12} E_{22} / E_{11}$	

Two sets of fiber orientations are considered. The fiber orientations in outer, central, and inner layers, respectively, are 1) $\theta^\circ, -\theta^\circ, 0^\circ$, 2) $\theta^\circ, -\theta^\circ, 90^\circ$ where θ assumes values ranging from 0° to 90° with 10-degree intervals. The two sets will be referred by notation 1- θ and 2- θ , and the numerical value of θ will indicate corresponding fiber orientation. For example, 1.20 corresponds to fiber orientation ($20^\circ, -20^\circ, 0^\circ$). When θ is zero, fibers are axially oriented, and when it is 90° the fibers are circumferentially oriented (Figure 4). The stiffness parameters α , β , etc., for these sets of fiber orientation may be found in Reference 17. The critical classical buckling load parameter σ_{cl} , buckling load $\bar{\sigma}_{cl}$, aspect ratio parameter μ and the circumferential wave number for small-deflection theory are given in Tables 1 and 2 for glass-epoxy and boron-epoxy composite cylindrical shells. These values are calculated with the aid of the computer program given in Reference 17.

To study the influence of initial geometric imperfections, the relative values of the initial imperfection amplitudes and parameters are set to

$$\overline{W}_1 = +4\overline{W}_2 = -4\overline{W}_3 = 16\overline{W}_4 \quad (34)$$

and

$$\overline{P}_1 = +4\overline{P}_2 = -4\overline{P}_3 = 16\overline{P}_4$$

These are the same as those given by Yoshimura buckling pattern (Reference 8). The imperfection ratio \overline{W}^* is defined here as the ratio of the sum of initial imperfection amplitudes to the thickness of the shell t . The following relation is obtained from Equations 27 and 34.

$$\overline{P}_4 = \frac{\overline{W}^* t}{\sqrt{a_{22} d_{22}^*}} \cdot \frac{1}{17}$$

For a specified value of \overline{W}^* the initial imperfection amplitude parameters \overline{P}_1 through \overline{P}_4 can be calculated from Equations 34 and 35.

For isotropic cylindrical shells all stiffness parameters given in Equation 27 are zero except that $\alpha/2 = P = \phi = 1$. Figure 3 shows the curves of the end-shortening parameter ϵ against the axial load parameter σ for an isotropic shell for different values of imperfection ratio \overline{W}^* . When \overline{W}^* is zero σ_{max} is equal to σ_{c1} which is equal to unity for the isotropic shell. In Reference 8, only two terms, corresponding to \overline{W}_1 and \overline{W}_2 are used in the assumed \overline{W} function to study the behavior of an isotropic shell. It is observed that for an isotropic shell the values of σ_{max} evaluated from the theory developed for anisotropic shells in this report are comparable to those given in Reference 8.

Figures 4 and 5 show the load-shortening curves for glass-epoxy and boron-epoxy composite cylindrical shells for fiber orientation $(0^\circ, 0^\circ, 0^\circ)$. In Tables 3 to 18, the values of σ_{max} , $\overline{\sigma}_{max}$, ρ^* and ϵ_{max} are given for $\overline{W}^* = 0.01, 0.02, 0.04, 0.06, 0.08, 0.1, 0.2, \text{ and } 0.3$ for glass-epoxy and boron-epoxy composite cylindrical shells. The same results are also presented in Figures 6 through 13. The discontinuity in the curves simply indicate that for that range of orientation there is no snap-through. Figure 6 gives the variation of $\overline{\sigma}_{max}$ with the fiber orientation $(\theta^\circ, -\theta^\circ, 0^\circ)$ for a three-layer, glass-epoxy composite. Figure 7 shows the variation of imperfection sensitivity ρ^* for the same

set. From these figures, it is evident that increase or decrease in classical buckling load with change in fiber orientation is generally accompanied by a decrease or increase in imperfection sensitivity. The same behavior can be observed in the case of a glass-epoxy composite for fiber orientation ($\theta, -\theta, 90^\circ$). From Figures 8, 9, 12, and 13 similar behavior is observed for boron-epoxy composite shells. In Figures 7, 9, 11, and 13 the values of ρ^* for isotropic shells are given for the purpose of comparison. It can be seen that the composite shells are less imperfection sensitive than isotropic shells and boron-epoxy composite shells are less imperfection sensitive than glass-epoxy composite shells.

REFERENCE

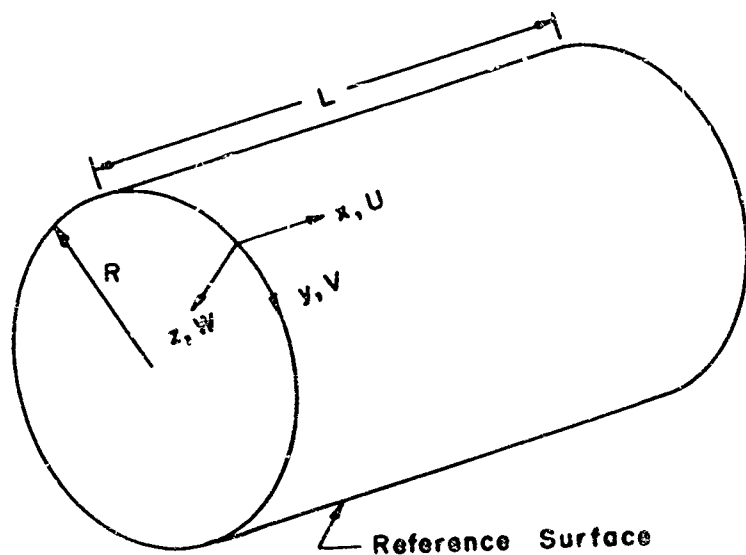
1. Flügge, W., "Die Stabilität der Kreiszyinderschale," Ingenieur-Archiv, Vol. 3, No. 5, p. 463, 1932.
2. Donnell, L.H., "A New Theory for the Buckling of Thin Cylinders Under Axial Compression and Bending," Transactions of the American Society of Mechanical Engineers, Vol. 56, , No. 11, p. 795, 1934.
3. Donnell, L.H., and Wan, C., "Effect of Imperfections on Buckling of Thin Cylinders and Columns Under Axial Compression," J. Appl. Mech., Vol. 17, No. 1, p. 73, 1950.
4. Loo, T.T., "Effects of Large Deflections and Imperfections on the Elastic Buckling of Cylinders Under Torsion and Axial Compression," Proceedings of the Second U.S. Congress of Applied Mechanics, p. 345, 1954.
5. Lee, L.H.N., "Effects of Modes of Initial Imperfections on the Stability of Cylindrical Shells Under Axial Compression," NASA-TN-D-1510, Washington, D.C., 1962, p. 143.
6. Sobey, A.J., "The Buckling of an Axially Loaded Circular Cylinder With Initial Imperfections," Royal Aeronautical Establishment Technical Report No. 64016, 1964.
7. Yang, P.B., and Jones, R.F., "An Analysis of Stability Critical Orthotropic Cylinders Subjected to Axial Compression," Presented at AIAA/ASME 8th Structures, Structural Dynamics and Materials Conference, Palm Springs, California (1967).
8. Madsen, W.A., and Hoff, N.J., "The Snap-Through and Postbuckling Equilibrium Behavior of Circular Shells Under Axial Load," SUDAER No. 227, Dept. Aero. and Astro., Stanford University (1965).
9. Ambartsumyan, S.A., "Theory of Anisotropic Shells," NASA-TT F-118 (1964).

REFERENCES (CONTD)

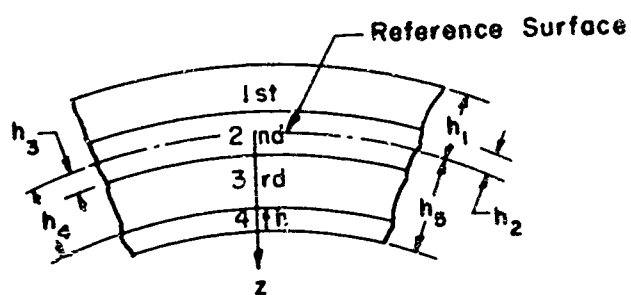
10. Dong, S.B., Pister, K.S., and Taylor, R.L., "On the Theory of Laminated Anisotropic Shells and Plates," J. Aero. Sci., Vol 29, No. 8, p. 968, 1962.
11. Tasi, J., Feldman, A., and Stang, D.A., "The Buckling Strength of Filament-Wound Cylinders Under Axial Compression," NASA-CR-266 (1965).
12. Holston, Jr., A., Feldman, A., and Stang, D.A., Stability of Filament-Wound Cylinders Under Combined Loading, AFFDL-TR-67-55 Air Force Flight Dynamics Laboratory, Wright-Patterson Air Force Base, Ohio (1967).
13. Cheng, S. and Ho, B.P.C., "Stability of Heterogeneous Aeolotropic Cylindrical Shells Under Combined Loading," AIAA J. 1, p. 892 (1963).
14. Ho, B.P.C. and Cheng, S., "Some Problems in Stability of Heterogeneous Aeolotropic Cylindrical Shells Under Combined Loading," AIAA J. 1, p. 1603 (1963).
15. Tasi, J., "Effects of Heterogeneity on the Stability of Composite Cylindrical Shells Under Axial Compression," AIAA J., 4, p. 1658 (1966).
16. Thurston, G.A., "On the Stability of Filament Wound Cylinders Under Axial Compression," Presented at 6th Annual Symposium, Filament Structures Technology, Albuquerque, New Mexico (1965).
17. Khot, N.S., On the Effects of Fiber Orientation and Nonhomogeneity on Buckling and Postbuckling Equilibrium Behavior of Fiber-Reinforced Cylindrical Shells Under Uniform Axial Compression, AFFDL-TR-68-19 Air Force Flight Dynamics Laboratory, Wright-Patterson Air Force Base, Ohio (1968).
18. Tsai, S.W., Mechanics of Composite Materials, AFML-TR-66-149 (Part II) Air Force Materials Laboratory, Wright-Patterson Air Force Base, Ohio (1966).

REFERENCES (CONTD)

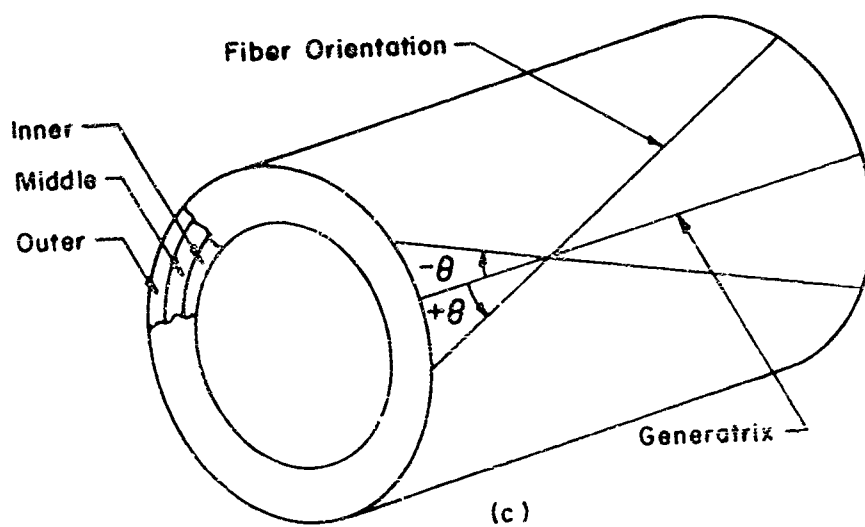
19. Almroth, B.O., "Postbuckling Behavior of Axially Compressed Circular Cylinders," AIAA J., 1. p. 630 (1963).
20. Koiter, W.T., "Elastic Stability and Post-Buckling Behavior," in Nonlinear Problems, edited by Langer, R.E., University of Wisconsin Press, Madison, Wisconsin (1963).
21. Hutchinson, J., "Axial Buckling of Pressurized Imperfect Cylindrical Shells," AIAA J., 3, p. 1461 (1965).
22. Hildebrand, F.B., Introduction to Numerical Analysis, McGraw-Hill, New York (1956).



(a)



(b)



(c)

Figure 1. Geometry

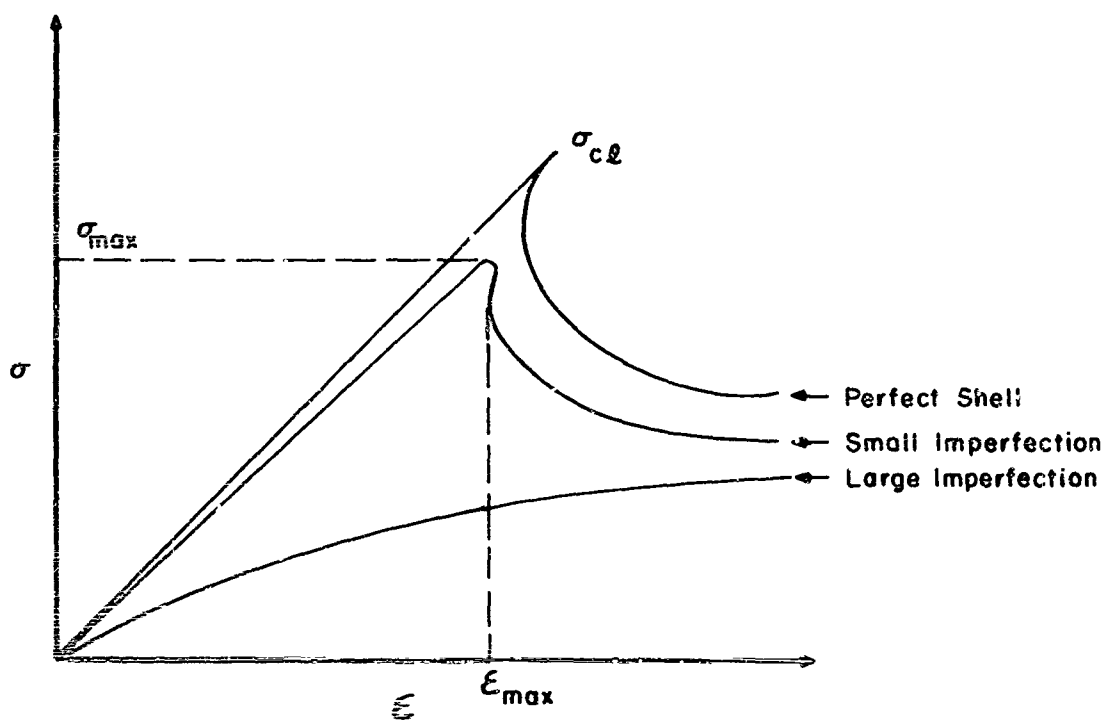


Figure 2. Notation

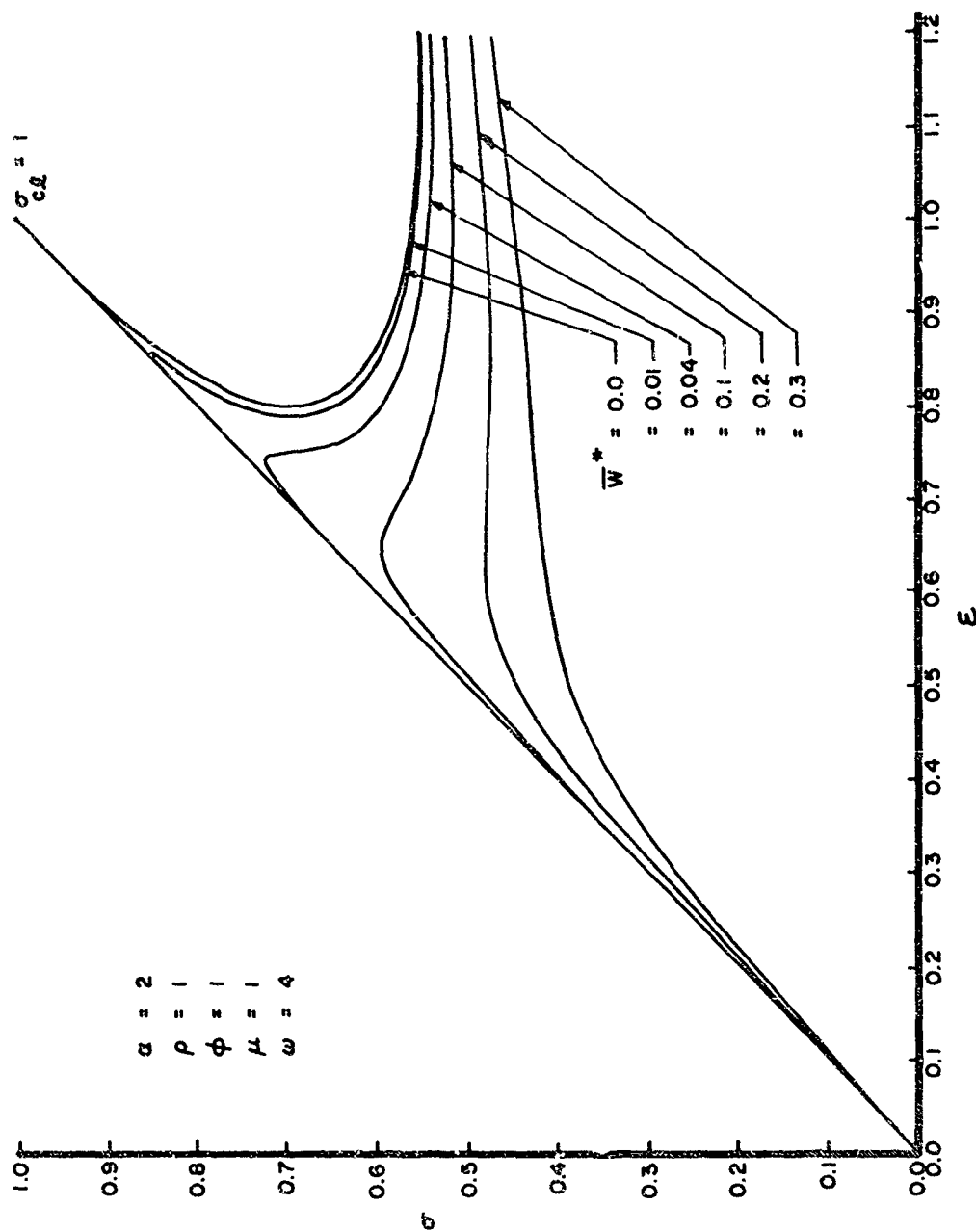


Figure 3. Initial Imperfection Solution of Isotropic Cylinder

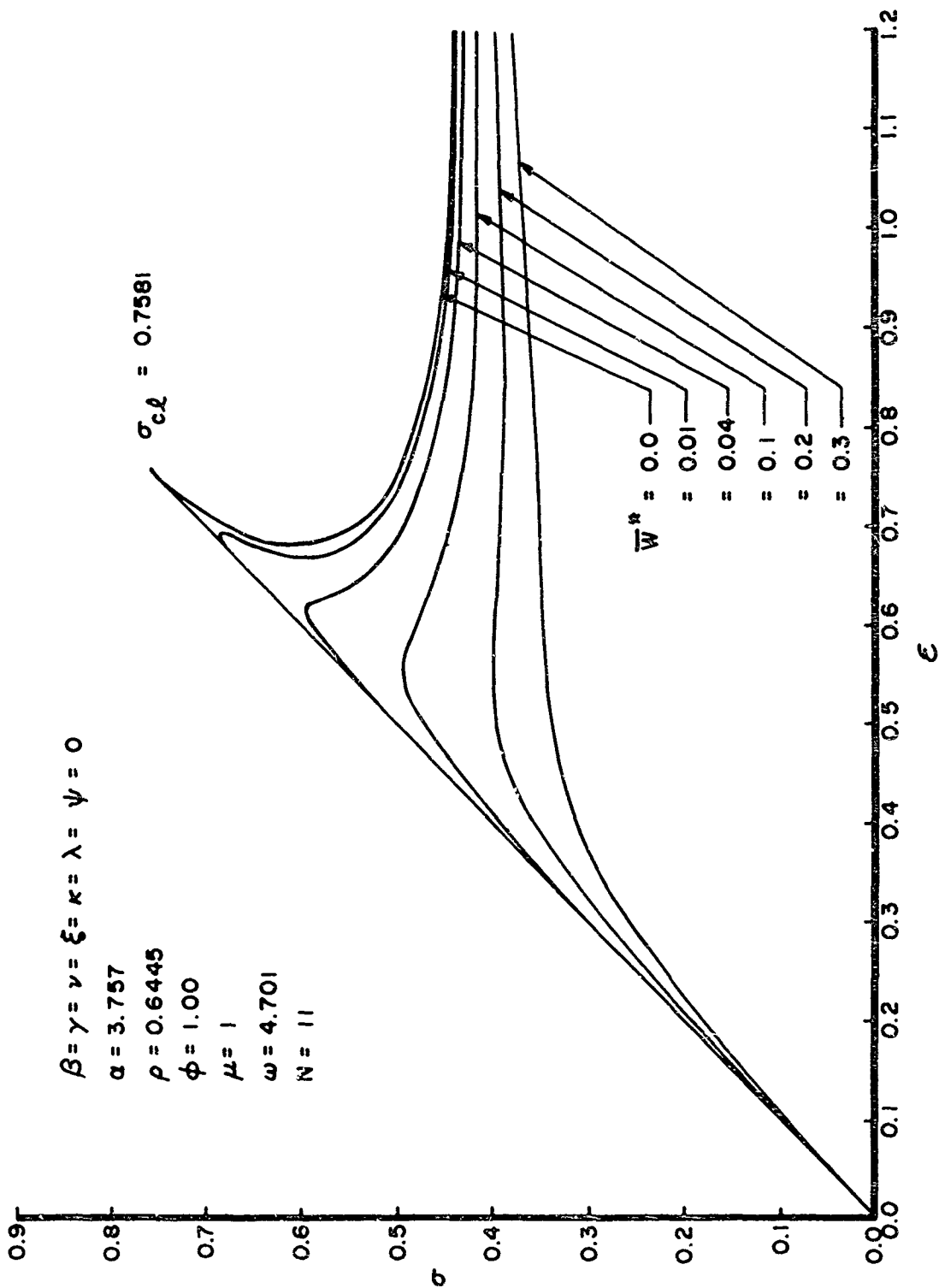


Figure 4. Initial Imperfection Solution of Glass-Epoxy Composite Cylinder for Fiber Orientation ($0^\circ, 0^\circ, 0^\circ$)

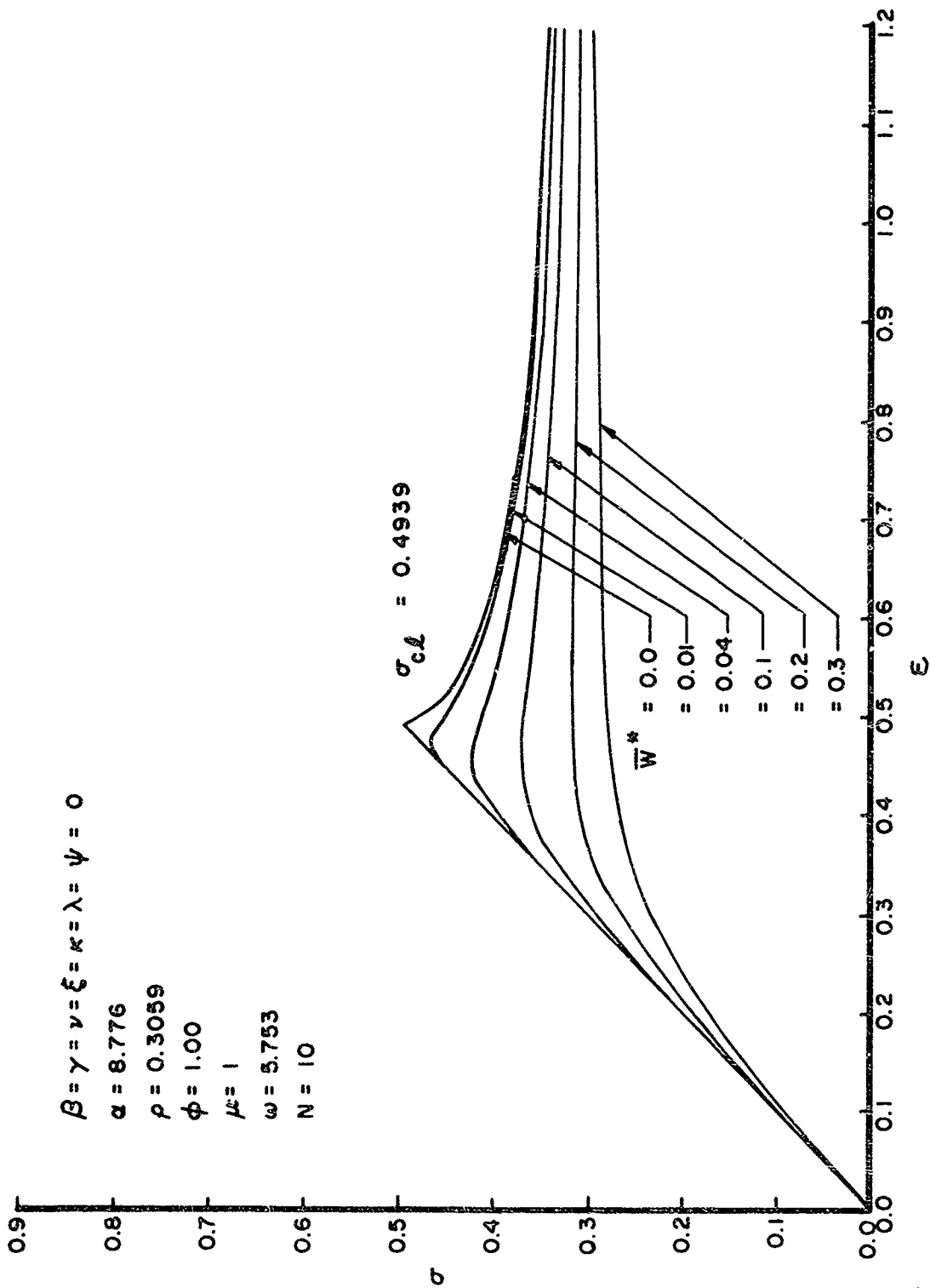


Figure 5. Initial Imperfection Solution of Boron-Epoxy Composite Cylinder for Fiber Orientation ($0^\circ, 0^\circ, 0^\circ$)

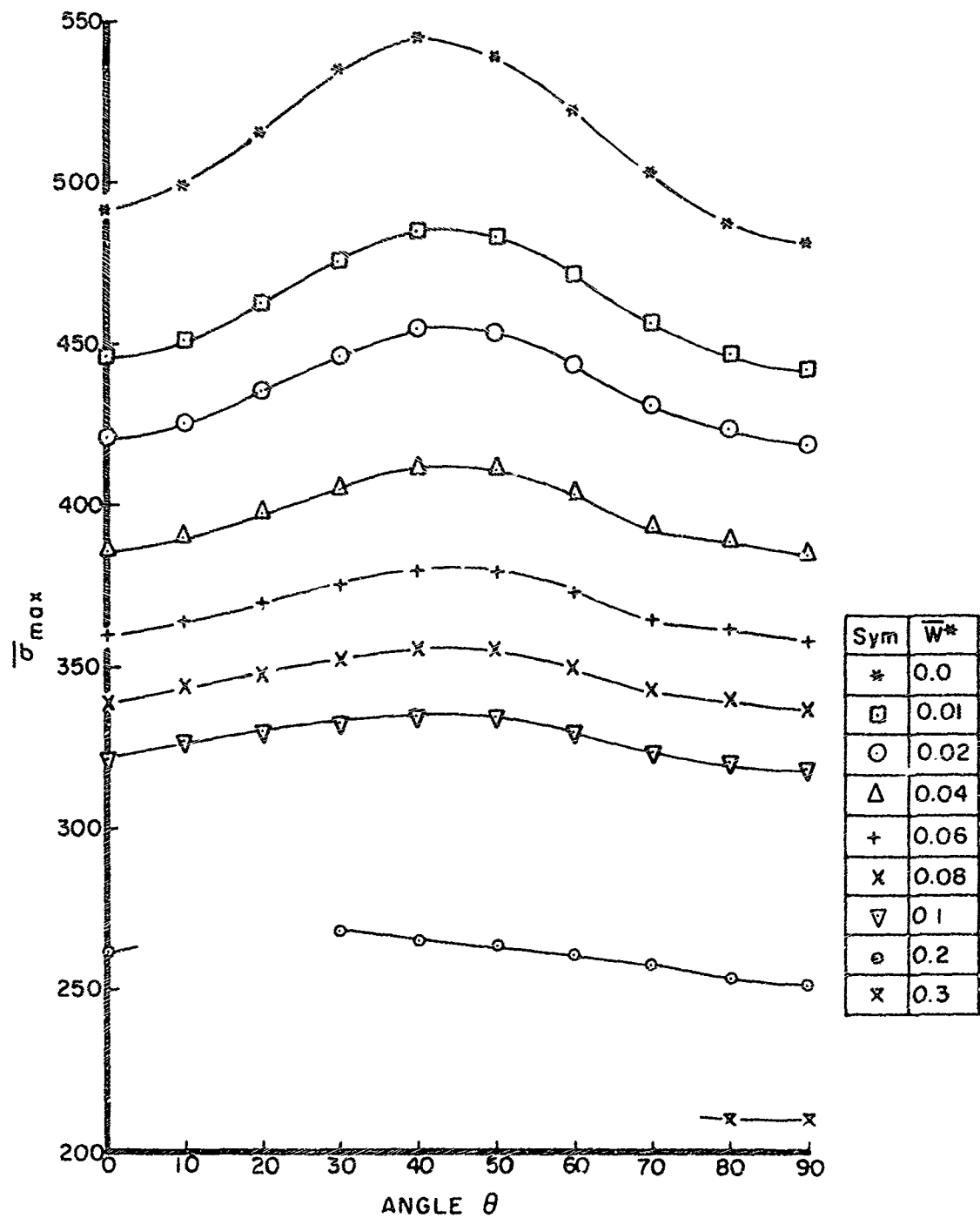


Figure 6. Influence of Initial Imperfection on Buckling Load of Three-Layer, Glass-Epoxy Composite Cylinder for Fiber Orientation (θ° , $-\theta^\circ$, 0°)

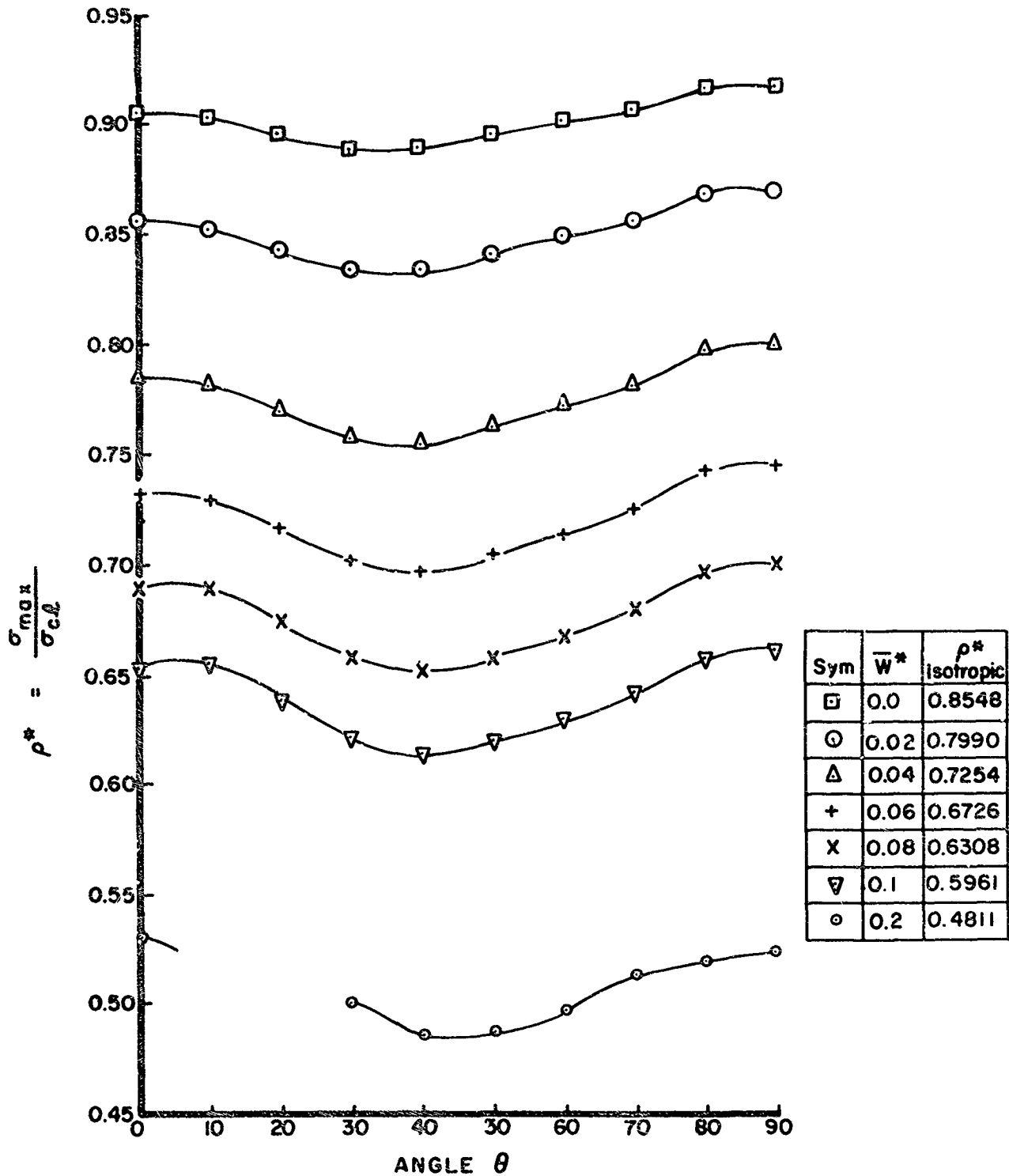


Figure 7. Imperfection Sensitivity of Three-Layer Glass-Epoxy Composite Cylinder for Fiber Orientation (θ° , $-\theta^\circ$, 0°)

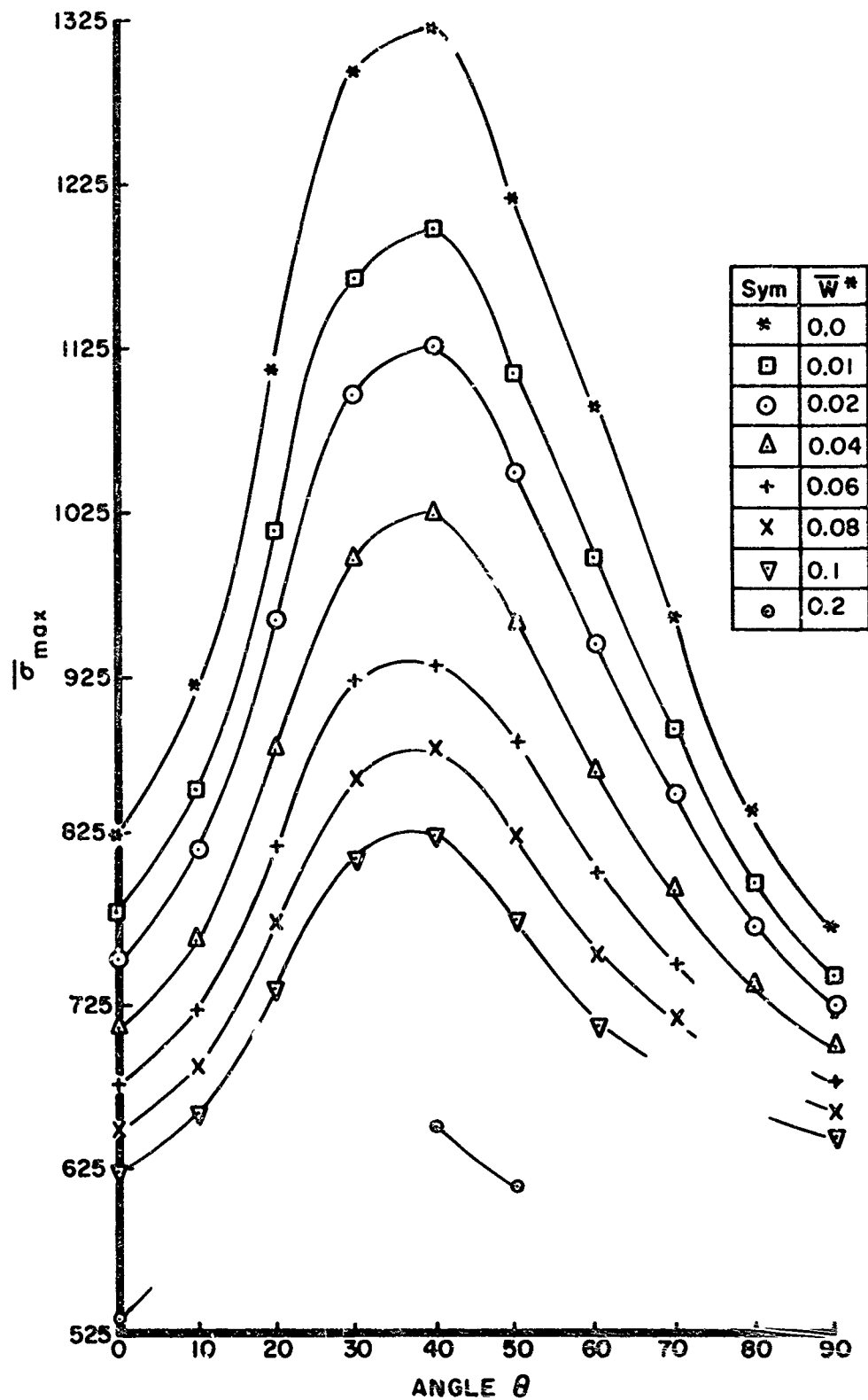


Figure 8. Influence of Initial Imperfection on Buckling Load of Three-Layer, Boron-Epoxy Composite Cylinder for Fiber Orientation ($\theta^\circ, -\theta^\circ, 0^\circ$)

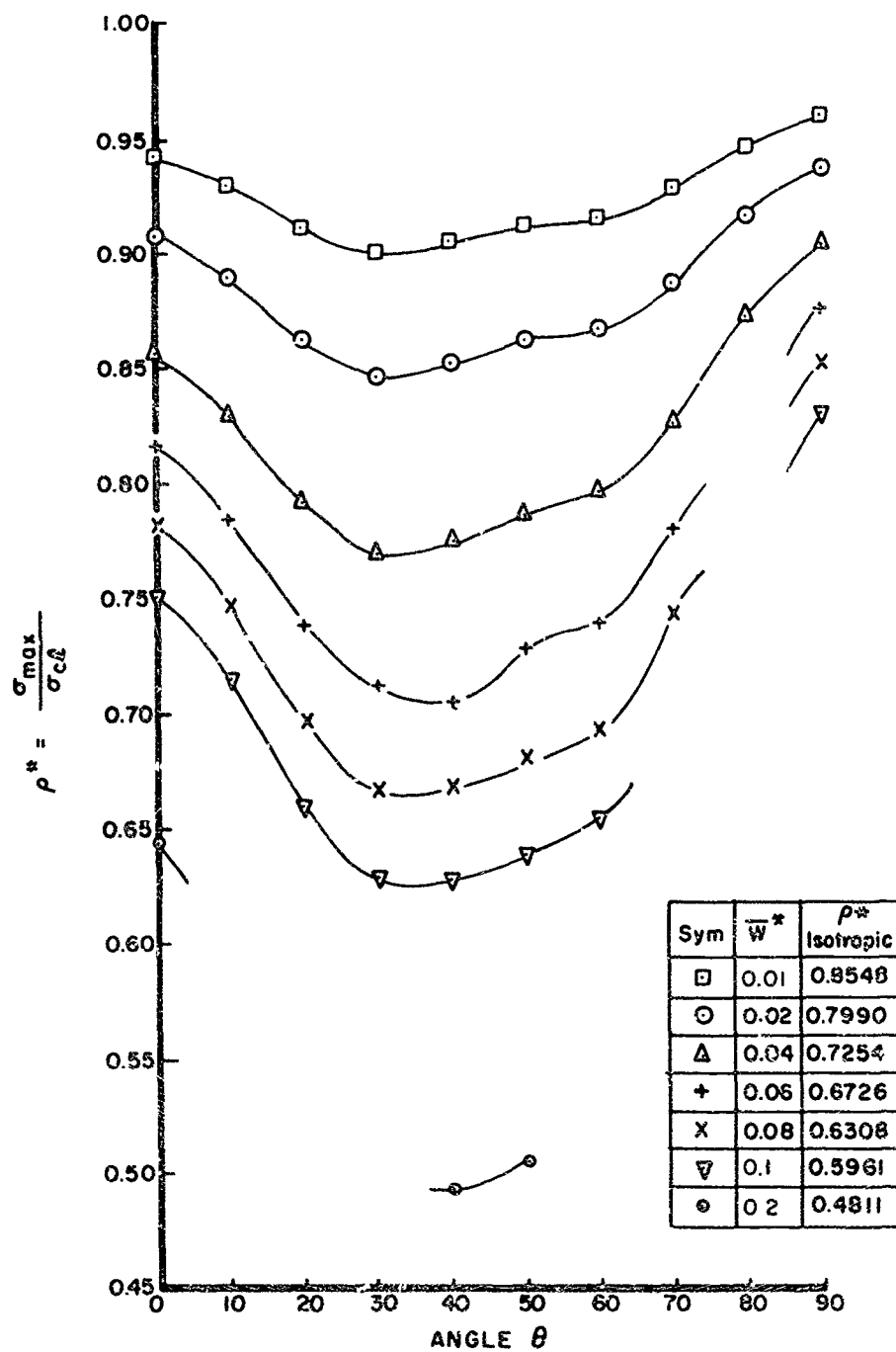


Figure 9. Imperfection Sensitivity of Three-Layer, Boron-Epoxy Composite Cylinder for Fiber Orientation ($\theta^\circ, -\theta^\circ, 0^\circ$)

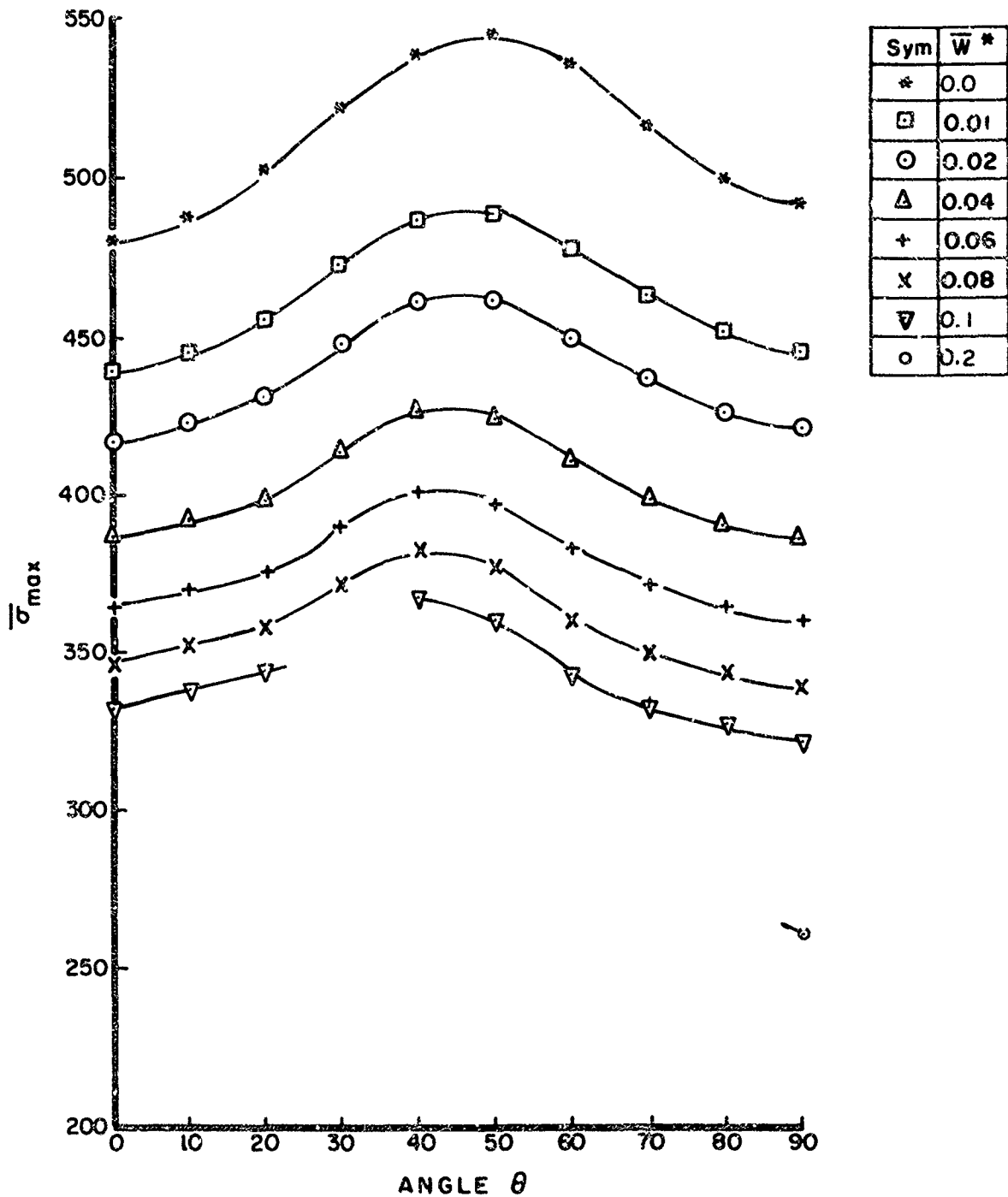


Figure 10. Influence of Initial Imperfection on Buckling Load of Three-Layer, Glass-Epoxy Composite Cylinder for Fiber Orientation ($\theta^\circ, -\theta^\circ, 90^\circ$)

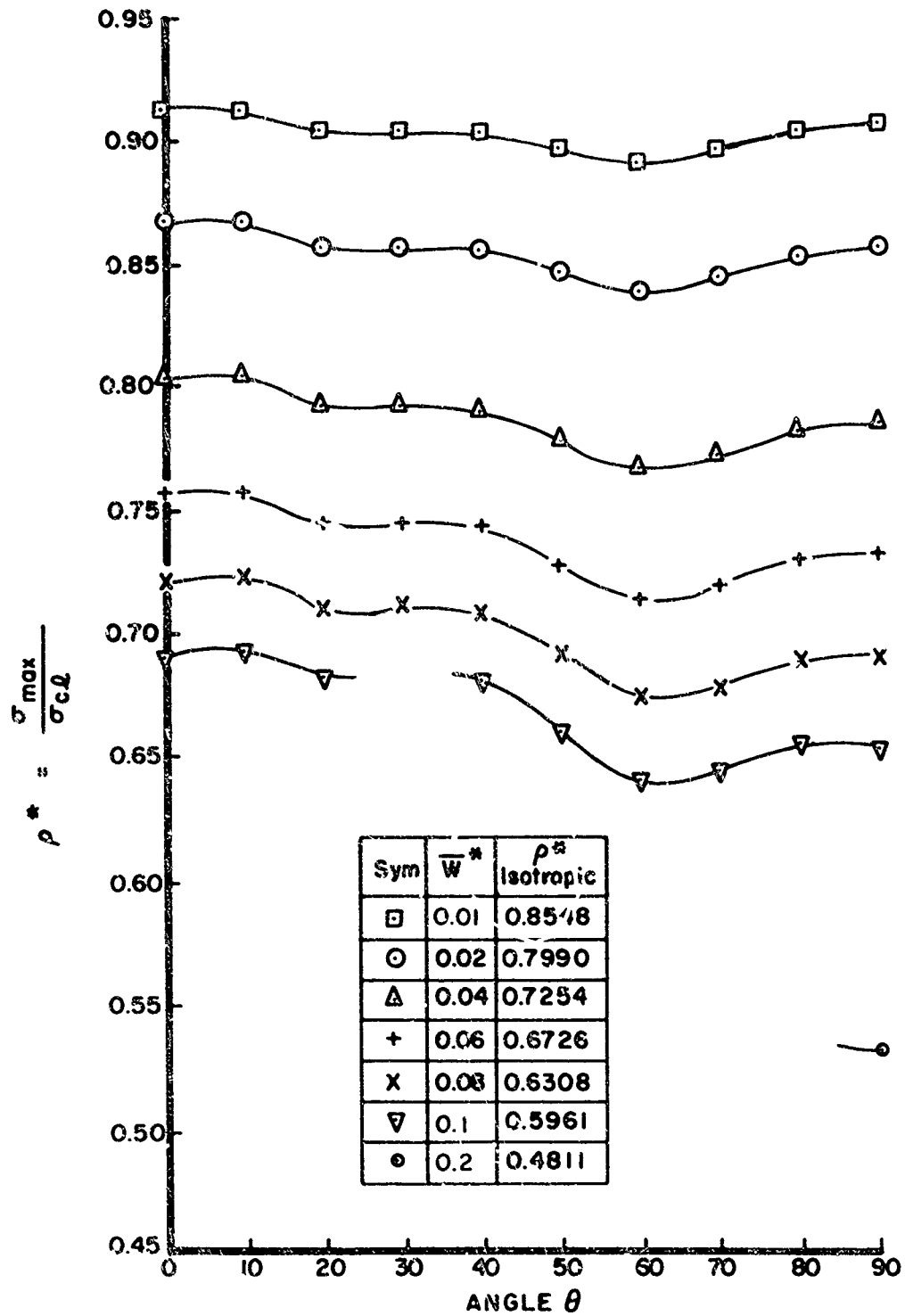


Figure 11. Imperfection Sensitivity of Three-Layer, Glass-Epoxy Composite Cylinder for Fiber Orientation (θ° : -6°, 90°)

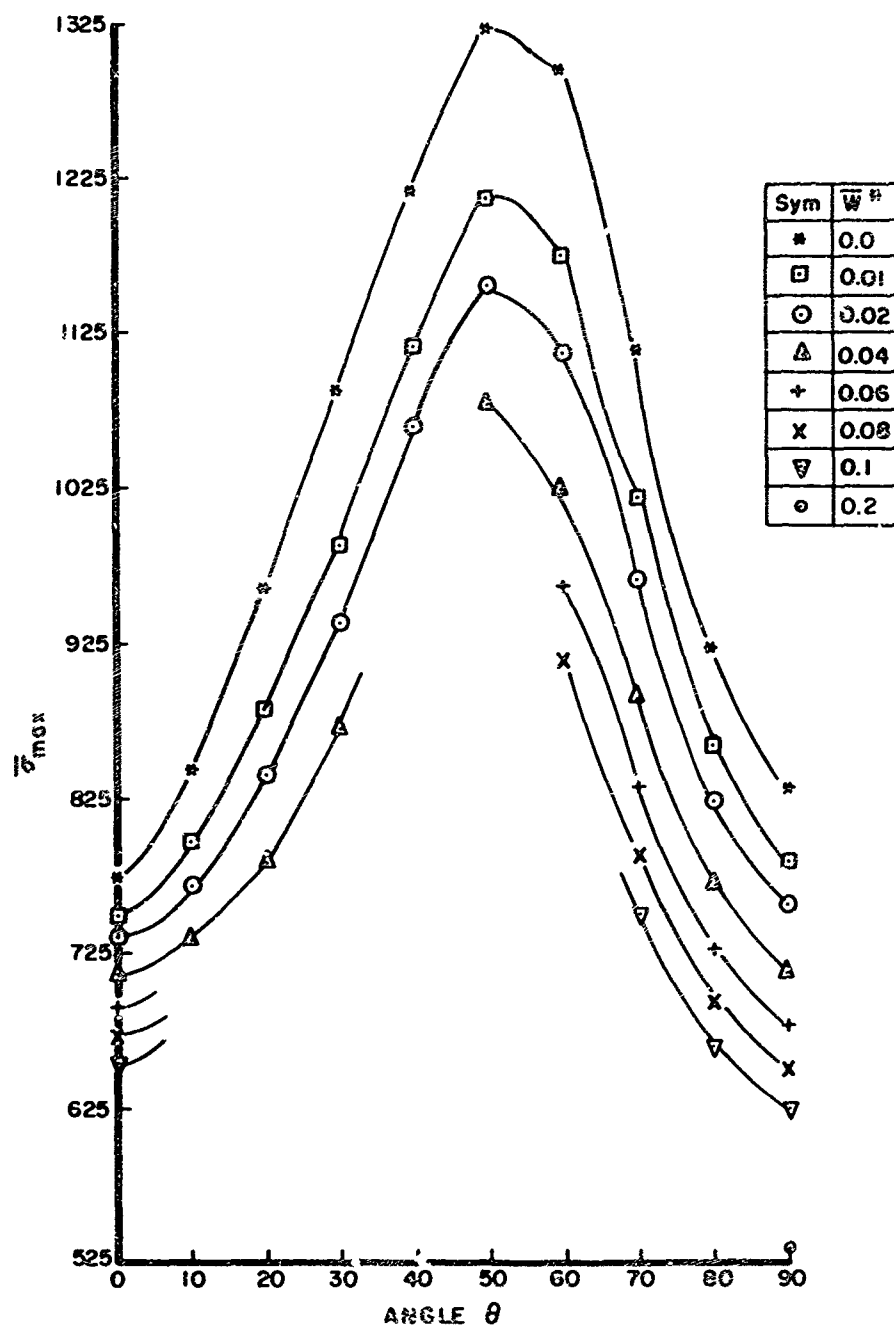


Figure 12. Influence of Initial Imperfection on Buckling Load of Three-Layer, Boron-Epoxy Composite Cylinder for Fiber Orientation (θ , $-\theta$, 90°)

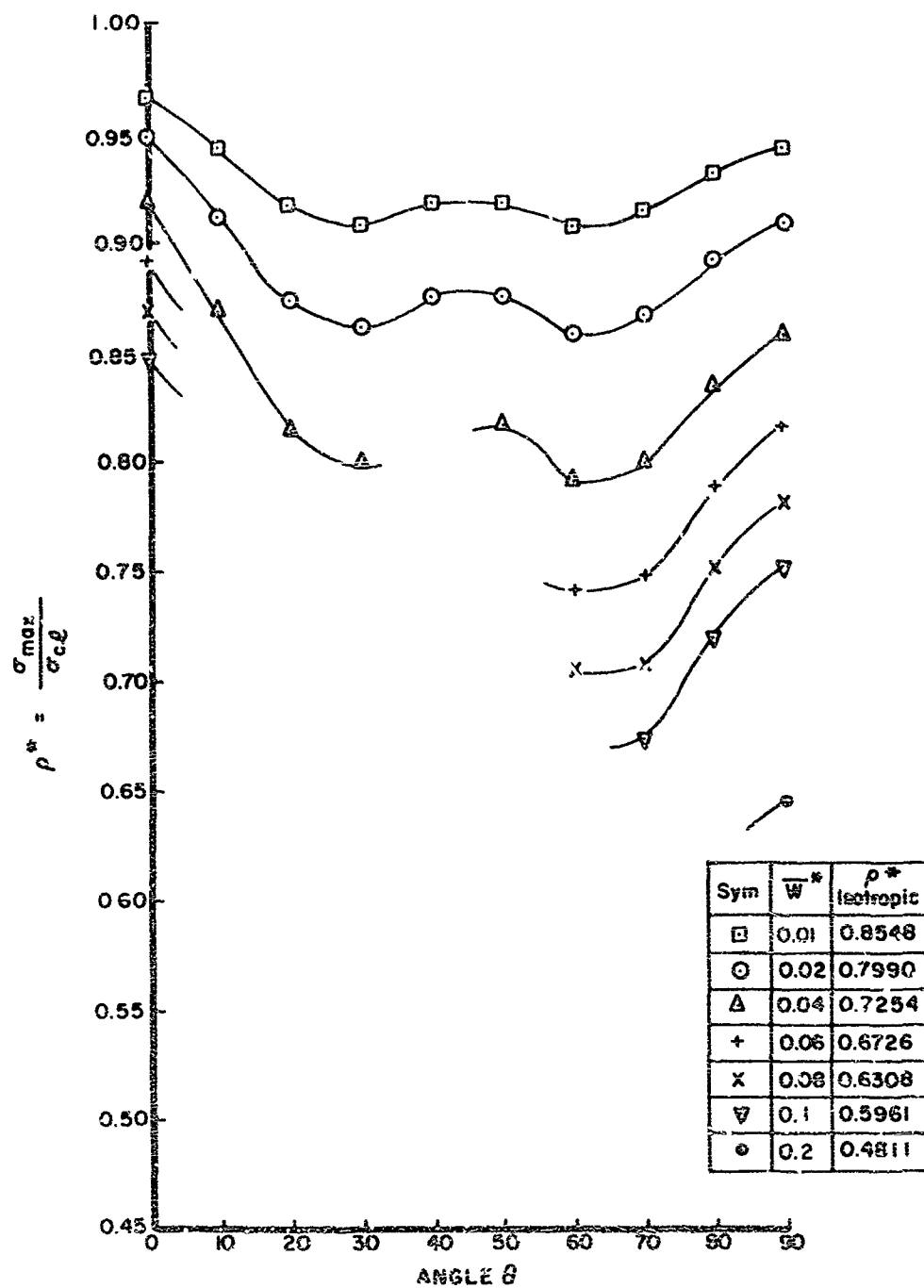


Figure 13. Imperfection Sensitivity of Three-Layer, Boron-Epoxy Composite Cylinder for Fiber Orientation (θ^* , $-\theta^*$, 90°)

TABLE 1.

CLASSICAL BUCKLING LOADS FOR GLASS-EPOXY
COMPOSITE CYLINDRICAL SHELL

CASE	σ_{cl}	$\bar{\sigma}_{cl}$	μ	N
1. 0	7.5808E-01	4.9158E 02	1.0000E 00	11
1.10	7.8154E-01	4.9907E 02	9.9740E-01	12
1.20	8.4265E-01	5.1599E 02	9.8253E-01	12
1.30	9.2255E-01	5.3507E 02	9.3027E-01	12
1.40	9.7893E-01	5.4473E 02	8.4374E-01	12
1.50	9.7384E-01	5.3874E 02	7.9899E-01	12
1.60	9.1645E-01	5.2222E 02	8.0312E-01	12
1.70	8.4230E-01	5.0295E 02	8.3260E-01	12
1.80	7.9227E-01	4.8750E 02	7.8663E-01	11
1.90	7.5748E-01	4.8055E 02	8.0854E-01	11
2. 0	6.8789E-01	4.8054E 02	1.2368E 00	11
2.10	7.1080E-01	4.8750E 02	1.2712E 00	11
2.20	7.7171E-01	5.0295E 02	1.2011E 00	12
2.30	8.5789E-01	5.2222E 02	1.2452E 00	12
2.40	9.3617E-01	5.3874E 02	1.2516E 00	12
2.50	9.6070E-01	5.4473E 02	1.1852E 00	12
2.60	9.1760E-01	5.3507E 02	1.0749E 00	12
2.70	8.4390E-01	5.1600E 02	1.0177E 00	12
2.80	7.8272E-01	4.9906E 02	1.0026E 00	12
2.90	7.5808E-01	4.9158E 02	1.0000E 00	11

TABLE 2.

CLASSICAL BUCKLING LOADS FOR BORON-EPOXY
COMPOSITE CYLINDRICAL SHELL

CASE	σ_{c0}	$\bar{\sigma}_{c0}$	μ	N
1. 0	4.9392E-01	8.2929E 02	1.0000E 00	10
1.10	5.6225E-01	9.2130E 02	1.0012E 00	11
1.20	7.3151E-01	1.1134E 03	9.7972E-01	12
1.30	9.4227E-01	1.2958E 03	8.7935E-01	13
1.40	1.0168E 00	1.3212E 03	7.4584E-01	13
1.50	9.1515E-01	1.2163E 03	7.2442E-01	13
1.60	7.6007E-01	1.0883E 03	7.9051E-01	13
1.70	6.0374E-01	9.6170E 02	8.9527E-01	13
1.80	4.5867E-01	8.4377E 02	9.4702E-01	12
1.90	3.7875E-01	7.7412E 02	9.6256E-01	11
2. 0	3.6541E-01	7.7412E 02	1.0389E 00	11
2.10	4.1170E-01	8.4378E 02	1.0559E 00	12
2.20	5.1807E-01	9.6170E 02	1.1170E 00	13
2.30	6.8294E-01	1.0883E 03	1.2650E 00	13
2.40	8.8459E-01	1.2164E 03	1.3804E 00	13
2.50	1.0151E 00	1.3212E 03	1.3407E 00	13
2.60	9.5486E-01	1.2958E 03	1.1372E 00	13
2.70	7.5876E-01	1.1133E 03	1.0207E 00	12
2.80	5.7806E-01	9.2131E 02	9.9877E-01	11
2.90	4.9392E-01	8.2929E 02	1.0000E 00	10

TABLE 3.

BUCKLING LOADS FOR IMPERFECT GLASS-EPOXY
COMPOSITE CYLINDRICAL SHELL FOR

$$\bar{w}^* = 0.01$$

CASE	σ_{\max}	$\bar{\sigma}_{\max}$	ρ^*	ϵ_{\max}
1. 0	6.8687E-01	4.4540E 02	9.0607E-01	6.9242E-01
1.10	7.0550E-01	4.5051E 02	9.0270E-01	7.1192E-01
1.20	7.5472E-01	4.6215E 02	8.9565E-01	7.5992E-01
1.30	8.1979E-01	4.7547E 02	8.8861E-01	8.2392E-01
1.40	8.7048E-01	4.8438E 02	8.8922E-01	8.7392E-01
1.50	8.7217E-01	4.8249E 02	8.9560E-01	8.7544E-01
1.60	8.2606E-01	4.7071E 02	9.0137E-01	8.2994E-01
1.70	7.6338E-01	4.5583E 02	9.0630E-01	7.6814E-01
1.80	7.1679E-01	4.4669E 02	9.1629E-01	7.2098E-01
1.90	6.9468E-01	4.4071E 02	9.1709E-01	6.9942E-01
2. 0	6.2799E-01	4.3870E 02	9.1292E-01	6.3844E-01
2.10	6.4861E-01	4.4485E 02	9.1251E-01	6.5969E-01
2.20	6.9812E-01	4.5499E 02	9.0464E-01	7.0812E-01
2.30	7.7536E-01	4.7198E 02	9.0380E-01	7.8594E-01
2.40	8.4515E-01	4.8636E 02	9.0277E-01	8.5562E-01
2.50	8.6120E-01	4.8831E 02	8.9643E-01	8.5942E-01
2.60	8.1782E-01	4.7689E 02	8.9126E-01	8.2417E-01
2.70	7.5655E-01	4.6259E 02	8.9649E-01	7.6242E-01
2.80	7.3679E-01	4.5065E 02	9.0299E-01	7.1342E-01
2.90	6.8674E 01	4.4515E 02	9.0596E-01	6.9192E 01

TABLE 4.

BUCKLING LOADS FOR IMPERFECT GLASS-EPOXY
COMPOSITE CYLINDRICAL SHELL FOR

$$\frac{W}{h} = 0.02$$

CASE	σ_{\max}	$\bar{\sigma}_{\max}$	ρ^*	ϵ_{\max}
1. 0	6.4900E-01	4.2085E 02	8.5611E-01	6.5934E-01
1.10	6.6603E-01	4.2531E 02	8.5220E-01	6.7812E-01
1.20	7.1020E-01	4.3489E 02	8.4282E-01	2.0920E-02
1.30	7.6875E-01	4.4587E 02	8.3329E-01	7.7742E-01
1.40	8.1533E-01	4.5369E 02	8.3288E-01	8.2192E-01
1.50	8.1846E-01	4.5278E 02	8.4045E-01	8.2492E-01
1.60	7.7707E-01	4.4280E 02	8.4791E-01	7.8392E-01
1.70	7.2004E-01	4.2995E 02	8.5485E-01	7.2842E-01
1.80	6.7936E-01	4.2337E 02	8.6845E-01	6.8676E-01
1.90	6.5882E-01	4.1796E 02	8.6975E-01	6.6642E-01
2. 0	5.9681E-01	4.1691E 02	8.6763E-01	6.1687E-01
2.10	6.1651E-01	4.2283E 02	8.6735E-01	6.3781E-01
2.20	6.6134E-01	4.3102E 02	8.5698E-01	6.8156E-01
2.30	7.3459E-01	4.4716E 02	8.5626E-01	7.5594E-01
2.40	8.0035E-01	4.6058E 02	8.5492E-01	8.2156E-01
2.50	8.1295E-01	4.6095E 02	8.4621E-01	8.3000E-01
2.60	7.6945E-01	4.4868E 02	8.3855E-01	7.8219E-01
2.70	7.1256E-01	4.3569E 02	8.4437E-01	7.2437E-01
2.80	6.6739E-01	4.2553E 02	8.5265E-01	6.7969E-01
2.90	6.4900E-01	4.2085E 02	8.5611E 01	6.5934E-01

TABLE 5.

BUCKLING LOADS FOR IMPERFECT GLASS-EPOXY
COMPOSITE CYLINDRICAL SHELL FOR

$$\bar{W}^{\#} = 0.04$$

CASE	σ_{\max}	$\bar{\sigma}_{\max}$	$\rho^{\#}$	ϵ_{\max}
1. 0	5.9523E-01	3.8598E 02	7.8518E-01	6.1562E-01
1.10	6.1091E-01	3.9011E 02	7.8167E-01	6.3531E-01
1.20	6.4857E-01	3.9715E 02	7.6968E-01	6.7000E-01
1.30	6.9807E-01	4.0487E 02	7.5667E-01	7.1341E-01
1.40	7.3874E-01	4.1108E 02	7.5464E-01	7.5192E-01
1.50	7.4257E-01	4.1080E 02	7.6252E-01	7.5492E-01
1.60	7.0698E-01	4.0286E 02	7.7143E-01	7.2042E-01
1.70	6.5750E-01	3.9260E 02	7.8060E-01	6.7384E-01
1.80	6.2365E-01	3.8865E 02	7.9723E-01	6.3692E-01
1.90	6.0549E-01	3.8413E 02	7.9935E-01	6.1984E-01
2. 0	5.5331E-01	3.8653E 02	8.0436E-01	5.9469E-01
2.10	5.7194E-01	3.9226E 02	8.0464E-01	6.1656E-01
2.20	6.1125E-01	3.9837E 02	7.9207E-01	6.5469E-01
2.30	6.7934E-01	4.1353E 02	7.9187E-01	7.2625E-01
2.40	7.3961E-01	4.2563E 02	7.9004E-01	7.8531E-01
2.50	7.4753E-01	4.2386E 02	7.7811E-01	7.8375E-01
2.60	7.0363E-01	4.1030E 02	7.6682E-01	7.3000E-01
2.70	6.5187E-01	3.9858E 02	7.7245E-01	6.7594E-01
2.80	6.1238E-01	3.9045E 02	7.8237E-01	6.3750E-01
2.90	5.9523E-01	3.8598E 02	7.8518E-01	6.1562E-01

TABLE 6.

BUCKLING LOADS FOR IMPERFECT GLASS-EPOXY
COMPOSITE CYLINDRICAL SHELL FOR

$$\bar{W}^* = 0.06$$

CASE	σ_{\max}	σ_{\max}	\bar{p}^*	ϵ_{\max}
1. 0	5.5524E-01	3.6005E 02	7.3243E-01	5.8656E-01
1.10	5.7060E-01	3.6437E 02	7.3010E-01	6.0906E-01
1.20	6.0370E-01	3.6967E 02	7.1643E-01	6.3750E-01
1.30	6.4738E-01	3.7547E 02	7.0173E-01	6.7437E-01
1.40	6.8234E-01	3.7969E 02	6.9703E-01	7.0516E-01
1.50	6.8640E-01	3.7972E 02	7.0484E-01	7.0534E-01
1.60	6.5463E-01	3.7303E 02	7.1431E-01	6.7500E-01
1.70	6.1055E-01	3.6457E 02	7.2486E-01	6.3500E-01
1.80	5.8062E-01	3.6183E 02	7.4222E-01	6.0000E-01
1.90	5.6429E-01	3.5799E 02	7.4496E-01	5.8531E-01
2. 0	5.2161E-01	3.6438E 02	7.5828E-01	5.8812E-01
2.10	5.3961E-01	3.7009E 02	7.5916E-01	6.1219E-01
2.20	5.7570E-01	3.7520E 02	7.4601E-01	6.4875E-01
2.30	6.4032E-01	3.8978E 02	7.4639E-01	7.2000E-01
2.40	6.9659E-01	4.0087E 02	7.4408E-01	7.7344E-01
2.50	7.0083E-01	3.9738E 02	7.2950E-01	7.5969E-01
2.60	6.5630E-01	3.8270E 02	7.1524E-01	6.9844E-01
2.70	6.0783E-01	3.7166E 02	7.2026E-01	6.4594E-01
2.80	5.7217E-01	3.6481E 02	7.3100E-01	6.1156E-01
2.90	5.5524E-01	3.6005E 02	7.3243E-01	5.8656E-01

TABLE 7.

BUCKLING LOADS FOR IMPERFECT GLASS-EPOXY
COMPOSITE CYLINDRICAL SHELL FOR

$$\bar{W}^H = 0.08$$

CASE	σ_{\max}	$\bar{\sigma}_{\max}$	ρ^*	ϵ_{\max}
1. 0	5.2289E-01	3.3907E 02	6.8976E-01	5.6562E-01
1.10	5.3849E-01	3.4386E 02	6.8901E-01	5.9281E-01
1.20	5.6800E-01	3.4781E 02	6.7406E-01	6.1563E-01
1.30	6.0669E-01	3.5187E 02	6.5762E-01	6.4406E-01
1.40	6.3786E-01	3.5494E 02	6.5159E-01	6.6625E-01
1.50	6.4115E-01	3.5469E 02	6.5837E-01	6.6687E-01
1.60	6.1227E-01	3.4889E 02	6.6809E-01	6.4031E-01
1.70	5.7246E-01	3.4182E 02	6.7964E-01	6.0562E-01
1.80	5.4496E-01	3.3961E 02	6.9664E-01	5.7063E-01
1.90	5.3016E-01	3.3634E 02	6.9990E-01	5.5812E-01
2. 0	4.9649E-01	3.4683E 02	7.2176E-01	5.9344E-01
2.10	5.1413E-01	3.5261E 02	7.2331E-01	6.2094E-01
2.20	5.4842E-01	3.5742E 02	7.1066E-01	6.6219E-01
2.30	6.1059E-01	3.7168E 02	7.1173E-01	7.3687E-01
2.40	6.6360E-01	3.8188E 02	7.0805E-01	7.8312E-01
2.50	6.6443E-01	3.7674E 02	6.9161E-01	7.5156E-01
2.60	6.1899E-01	3.6094E 02	6.7457E-01	6.7937E-01
2.70	5.7290E-01	3.5030E 02	6.7887E-01	6.2687E-01
2.80	5.4016E-01	3.4440E 02	6.9011E-01	5.9594E-01
2.90	5.2289E-01	3.3907E 02	6.8976E-01	5.6562E-01

TABLE 8.

BUCKLING LOADS FOR IMPERFECT GLASS-EPOXY
COMPOSITE CYLINDRICAL SHELL FOR

$$\bar{W}^* = 0.10$$

CASE	σ_{\max}	$\bar{\sigma}_{\max}$	ρ^*	ϵ_{\max}
1. 0	4.9563E-01	3.2139E 02	6.5380E-01	5.5094E-01
1.10	5.1189E-01	3.2688E 02	6.5498E-01	5.8469E-01
1.20	5.3838E-01	3.2967E 02	6.3891E-01	6.0156E-01
1.30	5.7282E-01	3.3223E 02	6.2091E-01	6.2187E-01
1.40	6.0037E-01	3.3408E 02	6.1329E-01	6.3719E-01
1.50	6.0317E-01	3.3368E 02	6.1937E-01	6.3625E-01
1.60	5.7660E-01	3.2856E 02	6.2917E-01	6.1250E-01
1.70	5.4036E-01	3.2266E 02	6.4153E-01	5.8312E-01
1.80	5.1436E-01	3.2054E 02	6.5752E-01	5.4656E-01
1.90	5.0089E-01	3.1777E 02	6.6126E-01	5.3594E-01
2. 0	4.7583E-01	3.3240E 02	6.9172E-01	6.1031E-01
2.10	4.9333E-01	3.3835E 02	6.9405E-01	6.4375E-01
2.20	5.2730E-01	3.4366E 02	6.8329E-01	7.1875E-01
2.30	**			
2.40	6.3811E-01	3.6721E 02	6.8162E-01	8.4156E-01
2.50	6.3505E-01	3.6008E 02	6.6103E-01	7.5969E-01
2.60	5.8832E-01	3.4306E 02	6.4115E-01	6.7031E-01
2.70	5.4404E-01	3.3265E 02	6.4467E-01	6.1656E-01
2.80	5.1366E-01	3.2751E 02	6.5625E-01	5.8844E-01
2.90	4.9563E-01	3.2139E 02	6.5380E-01	5.5094E-01

** NC SNAP-THROUGH

TABLE 9.

BUCKLING LOADS FOR IMPERFECT GLASS-EPOXY
COMPOSITE CYLINDRICAL SHELL FOR

$$\bar{W}^* = 0.20$$

CASE	σ_{\max}	$\bar{\sigma}_{\max}$	ρ^*	E_{\max}
1. 0	4.0216E-01	2.6078E 02	5.3050E-01	5.4406E-01
1.10	**			
1.20	**			
1.30	4.6152E-01	2.6768E 02	5.0027E-01	6.0875E-01
1.40	4.7439E-01	2.6398E 02	4.8460E-01	5.6906E-01
1.50	4.7434E-01	2.6241E 02	4.8708E-01	5.5656E-01
1.60	4.5536E-01	2.5948E 02	4.9687E-01	5.4500E-01
1.70	4.3167E-01	2.5776E 02	5.1249E-01	5.4406E-01
1.80	4.0524E-01	2.5254E 02	5.1803E-01	4.7531E-01
1.90	3.9663E-01	2.5162E 02	5.2362E-01	4.7406E-01
2. 0	**			
2.10	**			
2.20	**			
2.30	**			
2.40	**			
2.50	**			
2.60	**			
2.70	**			
2.80	**			
2.90	4.0216E-01	2.6078E 02	5.3050E-01	5.4406E-01

** NO SLAP-THROUGH

TABLE 10.

BUCKLING LOADS FOR IMPERFECT GLASS-EPOXY
COMPOSITE CYLINDRICAL SHELL FOR

$$\bar{W}^* = 0.30$$

CASE	σ_{\max}	$\bar{\sigma}_{\max}$	ρ^*	E_{\max}
1. 0	**			
1.10	**			
1.20	**			
1.30	**			
1.40	**			
1.50	**			
1.60	**			
1.70	**			
1.80	3.3696E-01	2.0999E 02	4.3075E-01	4.6313E-01
1.90	3.3176E-01	2.1047E 02	4.3798E-01	4.7531E-01
2. 0	**			
2.10	**			
2.20	**			
2.30	**			
2.40	**			
2.50	**			
2.60	**			
2.70	**			
2.80	**			
2.90	**			

** NO SNAP-THROUGH

TABLE 11.

BUCKLING LOADS FOR IMPERFECT BOKON-EPOXY
COMPOSITE CYLINDRICAL SHELL FOR

$$\bar{W}^* = 0.01$$

CASE	σ_{\max}	$\bar{\sigma}_{\max}$	ρ^*	ϵ_{\max}
1. 0	4.6542E-01	7.8144E 02	9.4230E-01	4.7625E-01
1.10	5.2287E-01	8.5677E 02	9.2996E-01	5.3187E-01
1.20	6.6635E-01	1.0142E 03	9.1092E-01	6.7317E-01
1.30	8.4789E-01	1.1660E 03	8.9984E-01	8.5292E-01
1.40	9.2045E-01	1.1960E 03	9.0524E-01	9.2442E-01
1.50	8.3492E-01	1.1097E 03	9.1233E-01	8.3992E-01
1.60	6.9680E-01	9.9771E 02	9.1676E-01	4.4200E-03
1.70	5.6065E-01	8.9306E 02	9.2863E-01	5.7531E-01
1.80	4.3423E-01	7.9881E 02	9.4672E-01	4.6000E-01
1.90	3.6357E-01	7.4309E 02	9.5992E-01	4.0438E-01
2. 0	3.5321E-01	7.4827E 02	9.6661E-01	4.4156E-01
2.10	3.8825E-01	7.9572E 02	9.4304E-01	4.1469E-01
2.20	4.7535E-01	8.8240E 02	9.1754E-01	4.9187E-01
2.30	6.2007E-01	9.8811E 02	9.0794E-01	6.3781E-01
2.40	8.1135E-01	1.1157E 03	9.1720E-01	8.3594E-01
2.50	9.3124E-01	1.2121E 03	9.1739E-01	9.5125E-01
2.60	8.6554E-01	1.1746E 03	9.0646E-01	8.7766E-01
2.70	6.9338E-01	1.0174E 03	9.1383E-01	7.0134E-01
2.80	5.3844E-01	8.5816E 02	9.3146E-01	5.4812E-01
2.90	4.6542E-01	7.8144E 02	9.4230E-01	4.7625E-01

TABLE 12.

BUCKLING LOADS FOR IMPERFECT BORON-EPOXY
COMPOSITE CYLINDRICAL SHELL FOR

$$\overline{w}^* = 0.02$$

CASE	σ_{\max}	$\overline{\sigma}_{\max}$	ρ^*	ϵ_{\max}
1. 0	4.4868E-01	7.5333E 02	9.0841E-01	4.6750E-01
1.10	5.0030E-01	8.1979E 02	8.8982E-01	5.1656E-01
1.20	6.3049E-01	9.5964E 02	8.6190E-01	6.4250E-01
1.30	7.9694E-01	1.0959E 03	8.4577E-01	6.4200E-03
1.40	8.6638E-01	1.1257E 03	8.5207E-01	7.3670E-02
1.50	7.8865E-01	1.0482E 03	8.6177E-01	7.9717E-01
1.60	6.5925E-01	9.4394E 02	8.6735E-01	6.6984E-01
1.70	5.3575E-01	8.5340E 02	8.8739E-01	5.6156E-01
1.80	4.2029E-01	7.7317E 02	9.1632E-01	4.6875E-01
1.90	3.5505E-01	7.2568E 02	9.3743E-01	4.3531E-01
2. 0	3.4655E-01	7.3417E 02	9.4839E-01	4.8906E-01
2.10	3.7532E-01	7.6922E 02	9.1163E-01	4.2844E-01
2.20	4.5249E-01	8.3996E 02	8.7341E-01	4.8500E-01
2.30	5.8790E-01	9.3685E 02	8.6084E-01	6.2406E-01
2.40	7.7401E-01	1.0643E 03	8.7499E-01	8.2563E-01
2.50	8.8743E-01	1.1550E 03	8.7423E-01	9.2719E-01
2.60	8.1911E-01	1.1116E 03	8.5783E-01	8.3937E-01
2.70	6.5743E-01	9.6462E 02	8.6645E-01	6.7219E-01
2.80	5.1568E-01	8.2189E 02	8.9209E-01	5.3281E-01
2.90	4.4868E-01	7.5333E 02	9.0841E-01	4.6750E-01

TABLE 13.

BUCKLING LOADS FOR IMPERFECT BORON-EPOXY
COMPOSITE CYLINDRICAL SHELL FOR

$$\frac{W}{W^*} = 0.04$$

CASE	σ_{\max}	$\bar{\sigma}_{\max}$	ρ^*	ϵ_{\max}
1. 0	4.2315E-01	7.1047E 02	8.5672E-01	4.5719E-01
1.10	4.6673E-01	7.6478E 02	8.3011E-01	4.9719E-01
1.20	5.7881E-01	8.8098E 02	7.9125E-01	6.0219E-01
1.30	7.2419E-01	9.9590E 02	7.6856E-01	7.4076E-01
1.40	7.8730E-01	1.0230E 03	7.7429E-01	8.0092E-01
1.50	7.1953E-01	9.5631E 02	7.8624E-01	7.3542E-01
1.60	6.0485E-01	8.6605E 02	7.9578E-01	6.2844E-01
1.70	4.9885E-01	7.9462E 02	8.2627E-01	5.4875E-01
1.80	4.0034E-01	7.3647E 02	8.7283E-01	5.1531E-01
1.90	3.4227E-01	6.9956E 02	9.0368E-01	4.9531E-01
2. 0	3.3537E-01	7.1048E 02	9.1779E-01	5.4281E-01
2.10	3.5769E-01	7.3309E 02	8.6881E-01	5.0562E-01
2.20	4.2141E-01	7.8227E 02	8.1342E-01	5.0062E-01
2.30	5.4551E-01	8.6930E 02	7.9877E-01	6.3844E-01
2.40	**			
2.50	8.2836E-01	1.0781E 03	8.1604E-01	9.2406E-01
2.60	7.5430E-01	1.0236E 03	7.8996E-01	7.9687E-01
2.70	6.0571E-01	8.8874E 02	7.9829E-01	6.3469E-01
2.80	4.8178E-01	7.6786E 02	8.3344E-01	5.1406E-01
2.90	4.2315E-01	7.1047E 02	8.5672E-01	4.5719E-01

** NO SNAP-THROUGH

TABLE 14.

BUCKLING LOADS FOR IMPERFECT BORON-EPOXY
COMPOSITE CYLINDRICAL SHELL FOR

$$\bar{W}^N = 0.06$$

CASE	σ_{max}	$\bar{\sigma}_{max}$	ρ^*	ϵ_{max}
1. 0	4.0299E-01	6.7662E 02	8.1590E-01	4.5281E-01
1.10	4.4093E-01	7.2251E 02	7.8422E-01	4.8656E-01
1.20	5.4018E-01	8.2218E 02	7.3845E-01	5.7625E-01
1.30	6.7089E-01	9.2260E 02	7.1199E-01	6.9906E-01
1.40	7.1765E-01	9.3249E 02	7.0579E-01	7.5098E-01
1.50	6.6619E-01	8.8541E 02	7.2796E-01	6.9031E-01
1.60	5.6222E-01	8.0501E 02	7.3970E-01	5.9687E-01
1.70	4.7113E-01	7.5046E 02	7.8035E-01	5.5187E-01
1.80	**			
1.90	3.3184E-01	6.7824E 02	8.7615E-01	5.4281E-01
2. 0	3.2564E-01	6.8987E 02	8.9116E-01	5.8750E-01
2.10	**			
2.20	**			
2.30	**			
2.40	**			
2.50	**			
2.60	7.0797E-01	9.6076E 02	7.4144E-01	7.7875E-01
2.70	5.6720E-01	8.3223E 02	7.4754E-01	6.1219E-01
2.80	4.5570E-01	7.2629E 02	7.8833E-01	5.0437E-01
2.90	4.0299E-01	6.7662E 02	8.1590E-01	4.5281E-01

** NO SNAP-THROUGH

TABLE 15.

BUCKLING LOADS FOR IMPERFECT BORON-EPOXY
COMPOSITE CYLINDRICAL SHELL FOR

$$\bar{W}^* = 0.08$$

CASE	σ_{max}	$\bar{\sigma}_{max}$	ρ^*	ϵ_{max}
1. 0	3.8602E-01	6.4813E 02	7.8154E-01	4.5281E-01
1.10	4.1975E-01	6.8780E 02	7.4655E-01	4.8281E-01
1.20	5.0906E-01	7.7482E 02	6.9590E-01	5.5937E-01
1.30	6.2804E-01	8.6367E 02	6.6652E-01	6.6719E-01
1.40	6.7882E-01	8.8204E 02	6.6760E-01	7.0594E-01
1.50	6.2252E-01	8.2737E 02	6.8024E-01	6.5312E-01
1.60	5.2721E-01	7.5488E 02	6.9363E-01	5.7406E-01
1.70	4.4974E-01	7.1639E 02	7.4492E-01	5.8844E-01
1.80	**			
1.90	3.2270E-01	5.5956E 02	8.5201E-01	5.8844E-01
2. 0	3.1696E-01	6.7148E 02	8.6741E-01	6.3500E-01
2.10	**			
2.20	**			
2.30	**			
2.40	**			
2.50	**			
2.60	6.7270E-01	9.1289E 02	7.0450E-01	7.8594E-01
2.70	5.3636E-01	7.8698E 02	7.0689E-01	6.0000E-01
2.80	4.3427E-01	6.9214E 02	7.5125E-01	5.0156E-01
2.90	3.8602E-01	6.4813E 02	7.8154E-01	4.5281E-01

** NO SNAP-THROUGH

TABLE 16.

BUCKLING LOADS FOR IMPERFECT BORON-EPOXY
COMPOSITE CYLINDRICAL SHELL FOR

$$\bar{w}^* = 0.10$$

CASE	σ_{max}	$\bar{\sigma}_{max}$	ρ^*	ϵ_{max}
1. 0	3.7129E-01	6.2339E 02	7.5172E-01	4.5625E-01
1.10	4.0179E-01	6.5837E 02	7.1461E-01	4.8469E-01
1.20	4.8310E-01	7.3531E 02	6.6041E-01	5.4969E-01
1.30	5.9248E-01	8.1477E 02	6.2878E-01	6.4406E-01
1.40	6.3786E-01	8.2882E 02	6.2732E-01	6.7281E-01
1.50	5.8541E-01	7.7805E 02	6.3969E-01	6.2437E-01
1.60	4.9766E-01	7.1257E 02	6.5476E-01	5.5844E-01
1.70	**			
1.80	**			
1.90	3.1454E-01	6.4288E 02	8.3047E-01	6.3875E-01
2. 0	3.0918E-01	6.5500E 02	8.4612E-01	6.9250E-01
2.10	**			
2.20	**			
2.30	**			
2.40	**			
2.50	**			
2.60	**			
2.70	5.1085E-01	7.4955E 02	6.7327E-01	5.9719E-01
2.80	4.1614E-01	6.6324E 02	7.1989E-01	5.0531E-01
2.90	3.7129E-01	6.2339E 02	7.5172E-01	4.5625E-01

** NO SNAP-THROUGH

TABLE 17.

BUCKLING LOADS FOR IMPERFECT BORON-EPOXY
COMPOSITE CYLINDRICAL SHELL FOR

$$\bar{W}^R = 0.20$$

CASE	σ_{\max}	$\bar{\sigma}_{\max}$	ρ^*	ϵ_{\max}
1. 0	3.1791E-01	5.3377E 02	6.4365E-01	5.2500E-01
1.10	**			
1.20	**			
1.30	**			
1.40	5.0212E-01	6.5244E 02	4.9382E-01	6.0187E-01
1.50	4.6213E-01	6.1420E 02	5.0498E-01	5.8187E-01
1.60	**			
1.70	**			
1.80	**			
1.90	**			
2. 0	**			
2.10	**			
2.20	**			
2.30	**			
2.40	**			
2.50	**			
2.60	**			
2.70	**			
2.80	**			
2.90	3.1791E-01	5.3377E 02	6.4365E-01	5.2500E-01

** NO SNAP-THROUGH

TABLE 18.

BUCKLING LOADS FOR IMPERFECT BORON-EPOXY
COMPOSITE CYLINDRICAL SHELL FOR

$$\bar{W}^* = 0.30$$

CASE	σ_{max}	$\bar{\sigma}_{max}$	ρ^*	ϵ_{max}
1. 0	**			
1.10	**			
1.20	**			
1.30	**			
1.40	**			
1.50	**			
1.60	**			
1.70	**			
1.80	**			
1.90	**			
2. 0	**			
2.10	**			
2.20	**			
2.30	**			
2.40	**			
2.50	**			
2.60	**			
2.70	**			
2.80	**			
2.90	**			

** NO SNAP-THROUGH

UNCLASSIFIED

Security Classification

DOCUMENT CONTROL DATA - R & D		
(Security classification of title, body of abstract and indexing annotation must be entered when the overall report is classified)		
1. ORIGINATING ACTIVITY (Corporate author)		2a. REPORT SECURITY CLASSIFICATION
Air Force Flight Dynamics Laboratory Wright-Patterson Air Force Base, Ohio 45433		Unclassified
		2b. GROUP
3. REPORT TITLE		
ON THE INFLUENCE OF INITIAL GEOMETRIC IMPERFECTIONS ON THE BUCKLING AND POSTBUCKLING BEHAVIOR OF FIBER-REINFORCED CYLINDRICAL SHELLS UNDER UNIFORM AXIAL COMPRESSION		
4. DESCRIPTIVE NOTES (Type of report and inclusive dates)		
September 1967 - May 1968		
5. AUTHOR(S) (First name, middle initial, last name)		
Khot, N. S.		
6. REPORT DATE	7a. TOTAL NO. OF PAGES	7b. NO. OF REFS
October 1968	67	22
8a. CONTRACT OR GRANT NO	8b. ORIGINATOR'S REPORT NUMBER(S)	
b. PROJECT NO 1473	AFFDL-TR-68-136	
c. Task No. 147306	9b. OTHER REPORT NO(S) (Any other numbers that may be assigned this report)	
d.		
10. DISTRIBUTION STATEMENT		
This document has been approved for public release and sale; its distribution is unlimited.		
11. SUPPLEMENTARY NOTES		12. SPONSORING MILITARY ACTIVITY
		Air Force Flight Dynamics Laboratory Wright-Patterson Air Force Base, Ohio 45433
13. ABSTRACT		
<p>The effect of initial geometric imperfections on the buckling and postbuckling behavior of composite cylindrical shells subjected to uniform axial compression is studied in this report. The solution is obtained by employing von Kármán-Donnell nonlinear strain-displacement relations and the principle of stationary potential energy. Numerical results are given for various fiber orientations in the three-layer shell consisting of either glass-epoxy or boron-epoxy composites, with different initial imperfections. Results indicate that the boron-epoxy composite shells are less imperfection sensitive than the glass-epoxy composite shells. Isotropic shells are found to be more imperfection sensitive than composite shells. It is noticed that the increase or decrease in the classical buckling load with change in fiber orientation is generally accompanied by a decrease or increase in imperfection sensitivity of the shell.</p>		

DD FORM 1473
1 NOV 65UNCLASSIFIED
Security Classification

UNCLASSIFIED

Security Classification

14	KEY WORDS	LINK A		LINK B		LINK C	
		ROLE	WT	ROLE	WT	ROLE	WT
	Buckling Composites Fiber Reinforced Material Circular Cylinders Initial Imperfections Axial Load Postbuckling Large-Deflection Analysis						

UNCLASSIFIED

Security Classification